DRIFT Version 3.7.3: Mathematical Model Description

ESR/UC000417/001/Issue 3

October 2015

ESR Technology
Engineering, Safety & Risk

Authorisation Sheet

Report Title:	DRIFT Version 3.7.3: Mathematical Model Description
Customer Reference:	
Project Reference:	ESR/UC000417
Report Number:	001
Issue:	Issue 3
Distribution List:	

Report Status	Key Changes	Author	Reviewed	Authorised
Draft A	Port to Word format. Inclusion of changes for 3.6.7: 1. Stationary and non-stationary initial instantaneous clouds 2. Change to time averaging for time-varying clouds	G Tickle		
Issue 1	Corrected typos	G Tickle	E Walton	N Ketchell
Issue 1b	Changed equation numbering to include chapter numbers	G Tickle	E Walton	N Ketchell
Issue 2	Changes for 3.7.2	G Tickle	E Walton	N Ketchell
Issue 3	Changes for 3.7.3	G Tickle	E Walton	N Ketchell

DRIFT Version 3.7.3: Mathematical Model Description

G A Tickle and J E Carlisle

ESR Technology Ltd

Date: 1 September 2015

DRIFT Version 3.7.3:
Mathematical Model Description

G A Tickle, BSc, PhD and J E Carlisle, MPhys, PhD
ESR Technology Ltd
Whittle House
410 The Quadrant
Birchwood Park
Warrington
WA3 6FW
UK

This report documents the mathematical model for Version 3.7.3 of the gas dispersion model DRIFT. DRIFT Version 3.7.3 includes a number of modelling enhancements over earlier versions. The main modelling enhancements are:

- Buoyant lift-off and rise following the recommendations in HSE Research Report RR629
- Incorporation of a momentum jet model, replacing the need to run a separate model such as EJECT
- Modelling of finite-duration and time-varying releases
- Extension of thermodynamic modelling to include multi-component mixtures

The mathematical modelling of these enhancements is described in this report. To incorporate the enhancements a completely new computer implementation of DRIFT has been coded in C++. This includes a new user interface which is described elsewhere (in the DRIFT Version 3 User Guide). Verification and validation testing of the new model are described elsewhere in the following reports:

- Comparison of DRIFT Version 3 Predictions with DRIFT Version 2 and Experimental Data, ESR Technology Report ESR/D1000846/STR01/Issue 3, June 2012
- Comparisons of Predictions from the Gas Dispersion Model DRIFT (Version 3) against URAHFREP Data, 2012, *to be published as an HSE Research Report*

This report and the work it describes were funded by the Health and Safety Executive. Its contents, including any opinions and/or conclusions expressed, are those of the authors alone and do not necessarily reflect HSE Policy.

HSE COPYRIGHT PAGE.

CONTENTS

1 INTRODUCTION

DRIFT [1], [2], [3], [4] was originally developed as a dense gas dispersion model for ground-based continuously and instantaneously released clouds. The model was developed for the Health and Safety Executive (HSE) to aid in the assessment of major loss of containment accidents for the UK regulatory regime (COMAH) and the land-use planning regime. In 2008 the current authors published a HSE contract research report [5] to describe how the DRIFT model equations could be extended to cover situations where buoyancy results in the lift-off and rise of the contaminant cloud from the ground. In addition to buoyant lift-off, [5] described the integration of momentum jet model equations into DRIFT. Subsequent to [5], the following additional enhancements were specified for including within the DRIFT model:

- Finite duration and time-varying releases
- Multi-component thermodynamics

During the course of developing and testing the new DRIFT model some, mostly minor, changes to the initial specification in [5] have been required. This report is therefore presented as an update to [5] to reflect the new mathematical model[1].

A main motivation for this work is the modelling of hydrogen fluoride (HF) dispersion. However, buoyant rise may also occur for spills of other substances which are either intrinsically buoyant or become buoyant. Examples are liquefied natural gas (LNG), which may become buoyant due to heat transfer from the ground, and liquefied ammonia which has an additional heat contribution from its heat of mixing with water. It is intended that the resultant model may also be applied to these situations.

The need to consider the lift-off phase for HF released under low wind speed conditions was demonstrated by studies under the EU URAHFREP project [6]. That project considered a wide range of aspects affecting the behaviour of HF releases, including complex thermodynamics and buoyant lift-off. Studies under URAHFREP [6], employing simple models, demonstrate the potential for extending DRIFT-like models to describe plume lift-off behaviour. URAHFREP also included wind-tunnel studies on the lift-off behaviour of buoyant puffs and plumes [7], [8], yielding useful data for developing/validating models.

Although DRIFT was modified under URAHFREP, this related mainly to changes in the thermodynamic model, enhanced dilution of the ground based cloud and a revised 'lift-off criterion' value. These changes extended the usefulness of the model, and indicate that lift-off is expected to occur for cloud sizes encountered in risk assessments of HF facilities. However, in order to quantify the potential reduction in hazard range due to lift-off, the ground based dispersion model DRIFT needed to be extended to include elevated buoyant plume and puff dispersion.

This report is structured as follows:

Section 1: Introduction
Section 2: A summary of buoyant lift-off and rise relevant to extending DRIFT
Section 3: Changes to DRIFT's atmospheric model

[1] *Henceforth we will often refer to the previous DRIFT model as DRIFT v2 and the new version as DRIFT v3.*

Section 4:	Changes to DRIFT's instantaneous model
Section 5:	Changes to DRIFT's continuous model
Section 6:	The extension of DRIFT to deal with finite duration and time-varying releases
Section 7:	Changes to DRIFT's thermodynamics model
Section 8:	Discussion
Section 9:	Acknowledgements
Appendix A :	Details of how to compare DRIFT's results against toxic and flammable criteria
Appendix B :	Details of the extension of Wheatley's passive model to elevated sources

2 BUOYANT LIFT-OFF AND RISE

In this section we summarise previous work on modelling of buoyant lift-off and rise. This is not intended to form a comprehensive review of all available approaches, but to concentrate on those most relevant to extending DRIFT. It is useful here to consider separately the process of lift-off, by which we mean the transition from ground-based to elevated cloud, from the process of buoyant rise of a completely elevated cloud.

2.1 BUOYANT LIFT-OFF

2.1.1 Continuous releases

Buoyant lift-off models are reviewed in [9]. For a buoyant cloud to lift-off[2] it is necessary for the vertical rate of rise of the cloud to exceed the vertical rate of growth. Briggs [10] discussed these competing effects and introduced the idea of a 'critical lift-off' parameter to mark the boundary between ground-based buoyant and lifted-off buoyant clouds. Clouds with Richardson number Ri_* much less than the critical value are assumed to remain ground-based, whereas those with much higher values are assumed to lift-off. Here

$$Ri_* = \frac{g(\rho_a - \rho)H}{\rho_a u_*^2} \tag{2-1}$$

H is the vertical extent of the cloud, g the acceleration due to gravity, u_* is the friction velocity, ρ is the cloud density and ρ_a the air density. Briggs [10] initially estimated a critical value of 2 for plumes, but is understood [9] to have revised this to 29 in a subsequent unpublished paper.

Wind-tunnel experiments (*e.g*. those of Hall *et al.* [7]) indicate a smooth transition between ground-based and lifted-off plumes. Hanna *et al.* [11] provide a simple continuous model, based upon a fit to the warehouse fire wind-tunnel experiments of Hall *et al.* [12], [13]. However, the applicability of this approach to non-buoyancy conserving flows (as for HF) is very questionable.

Comparison of the predictions of a simple integral plume model [14] with the wind-tunnel experiments of Hall *et al.* [7] indicates good agreement for all but the wide sources. This simple integral model includes the effect of the ground merely as a truncation of the plume cross-section. For the wide sources the simple integral model over-predicts lift-off and modifications to suppress lift-off using the vertical momentum equation were found to have a detrimental effect on concentration predictions. This detrimental effect was believed to be due to the direct coupling between the vertical plume velocity and the 'buoyant' entrainment term. Alternative methods of suppressing plume rise from wide sources are required.

[14] also derived a buoyant correction to entrainment that is included within DRIFT's ground-based model. This buoyant correction is numerically similar to other published models [15], [16] and fits the URAHFREP data of Hall *et al.* [7]. DRIFT uses this buoyant correction up to a Richardson number where the URAHFREP data indicates that the wind-tunnel plumes completely lift-off.

---

[2] *By 'lift-off' here we mean the rise of the concentration maximum from ground-level*

Ott [17] also presents an integral plume model with the cross-section truncated by the ground. Conceptually Ott's model is similar to the simple integral model in [9], although it includes HF thermodynamics, a more sophisticated passive model and includes 'added mass' in the vertical momentum equation. Ott's model compares favorably with the URAHFREP field trial data [17], although it is recognised this data is dominated by passive behaviour. Ott's model was not compared with the URAHFREP wind-tunnel data. [17] suggests an alternative 'added mass' model that might provide a mechanism for suppressing lift-off of ground-based clouds.

EJECT [18] is a momentum jet model which includes HF thermodynamics and may be used as a source term for DRIFT v2. EJECT includes an elevated jet model that can in principle model buoyant as well as dense jets. When the elevated jet impinges on the ground, a sudden transition is made to a ground-based jet model [19], or if the jet has slowed sufficiently, EJECT writes a DRIFT input file. EJECT's ground-based jet model includes a buoyant enhancement based on that given in [14]. However, EJECT does not model elevated passive plumes and there is no provision for the grounded plume to lift-off.

2.1.2 Instantaneous releases

There is little information available for modelling the transition from ground based to elevated puffs.

Briggs [10] argues that the 'critical lift-off parameter' for puffs should be about 50% higher than for plumes due to the more diffusive inflow, but as acknowledged by Briggs, the arguments leading to this are somewhat speculative.

The URAHFREP experiments of Hall *et al.* [8] on buoyant puffs provide data on lift-off of short duration buoyant releases. These experiments show the increased variability of puffs as compared with continuous plumes. The URAHFREP puff experiments may be useful for model validation purposes, however *a priori* it is difficult to construct a mathematical model of puff lift-off directly from these.

2.2 BUOYANT RISE

2.2.1 Continuous releases

Due to the wide variety of applications, there are many published models and reviews covering the elevated dispersion of buoyant plumes (see e.g. [20]). Often plume rise is calculated to determine the effective source height for subsequent passive dispersion ignoring passive dilution during the rise phase. Many integral models use the same entrainment models for jets and plumes, although some differ (*e.g.* the model of Schatzmann [21] includes a densimetric Froude number dependence). Only a few models specifically include HF thermodynamics (see *e.g.* [16], [22], [18]).

Rising buoyant plumes have a characteristic kidney shaped cross-section resulting from the establishment of counter-rotating vortices. These vortices are efficient at mixing air with the plume. Most integral plume models include the effect of this enhanced mixing via empirical 'cross-flow' entrainment terms, but do not model the distortion of the cross-section, assuming axisymmetry.

In stable atmospheric conditions buoyant rise will be limited due to the decreasing atmospheric density with height. Conversely in unstable conditions buoyant rise may be enhanced. To account for this it is necessary to include the variation of temperature with height. Even though the effect on absolute temperature is small, the vertical gradient of atmospheric pressure affects the density gradient and hence the static stability. Plume rise models usually account for this by using potential temperature[3] in place of temperature.

Unstable conditions are characterised by thermal updraughts, balanced by downdraughts. This can lead to looping behaviour of elevated plumes, with the downdraughts bringing higher concentrations to the surface. In Gaussian passive dispersion models this effect can be included empirically by an increase in the standard deviation, σ_z of the vertical concentration. However, the instantaneous plume profile is less spread than this and including the enhanced vertical spread as a dilution can lead to buoyant plume rise being under-predicted [17].

Ground-based dispersion generally occurs within the lowest 10% of the atmospheric boundary layer - called the surface layer. DRIFT [1], [2] currently uses atmospheric profiles of wind speed and diffusivity in this layer. Buoyant releases may rise above the surface layer into the rest of the turbulent boundary layer. Scaling models exist for the whole boundary layer, but these are less well established than for the surface layer. [23] presents atmospheric profiles of wind speed and diffusivity based on scaling regions above the surface layer.

Generally dispersing material is trapped within the turbulent atmospheric boundary layer. [24] presents a model for dispersion from very buoyant sources, as might occur in large fires, including a model for plume penetration of an elevated inversion above the boundary layer. The passive dispersion models ADMS [25] and AERMOD [26] also include models for predicting buoyant penetration of an elevated inversion. These models require information on the strength of the elevated inversion.

2.2.2 Instantaneous releases

The literature on the rise of buoyant puffs is much less extensive than buoyant plumes. The behaviour of buoyant puffs has been studied by Richards [27], [28] and later Turner [29], [30], [31], [32], [33] who developed an integral model based on an entrainment hypothesis (relating the dilution of the puff to its vertical velocity). Turner's integral model forms the basis of fireball rise models [34], dispersion models from open-burn and explosives detonation (e.g. [35], [36]), elevated dense puff models [15] and chemically reacting puff models [37] (e.g. for UF6 dispersion). Deaves and Hebden [38] also review puff models in the context of dispersion following explosive releases.

Turner's model includes 'added mass' and in [31] he shows that a buoyant vortex model can be written in terms of an entraining spheroidal puff if added mass is included. Others, as indicated in [34], do not include added mass.

Generally the integral models for buoyant puff rise adopt uniform (top-hat) profiles and do not include the effects of ambient turbulence. Also the models assume that the puff is initially elevated and do not model lift-off behaviour or interaction with the ground.

---

[3] *Potential temperature is defined as the temperature of the air if taken isentropically to a reference pressure.*

2.3 PASSIVE DISPERSION

2.3.1 Wheatley's model

The DRIFT passive model is based on that of Wheatley [39]. Wheatley's model is for the diffusion of a passive puff released at the ground into a turbulent stratified shear flow. The model for mixing in the vertical is based on gradient-transfer or 'K-theory' and is an approximate solution of the diffusion equation for arbitrary power law profiles of atmospheric diffusivity and wind speed. The model accounts for the effect of wind shear and vertical mixing on longitudinal diffusion and distortion of the puff. The diffusivity and wind speed profiles adopted by DRIFT are those due of Businger [40]. A Gaussian model is adopted for horizontal dispersion using an approach due to Pasquill and Smith which relates the rate of lateral puff growth to the cross-wind turbulence intensity. Wheatley's approximate solution has vertical concentration profiles of the general form

$$F_v(z) = \exp[-(z/a)^s] \tag{2-2}$$

where s is related to the power law index for diffusivity and a is a measure of the vertical extent. The vertical profile is Gaussian ($s = 2$) when the diffusivity is constant with height (which is not the case near the ground) and exponential ($s = 1$) in neutral atmospheric stability.

Appendix 6 of [39] shows how Wheatley's passive model may be generalised for an elevated point source. The solution for the elevated source is more complex than for the ground-level source, but may be written in terms of the modified Bessel function of the first kind I_ν and the confluent hypergeometric function M.[4] For constant diffusivity and wind speed, the elevated passive model is exactly equivalent to a Gaussian model with reflection at the ground.

The solution given by Wheatley is for a no-flux boundary condition at the ground. In Appendix B we show that solution under more generalised boundary conditions is possible, e.g. to include a no-flux boundary condition at the mixing height, or to allow flux from the boundaries. However, the solutions with such generalised boundary conditions no longer appear to be readily expressible in terms of special functions and require numerical solution.

Brown *et al.* [41] compared the predictions of a K-theory model with field and laboratory measurements for both ground-level and elevated passive sources. The K-theory model evaluated by Brown *et al.* is almost identical to Wheatley's elevated passive solution. They found that the K-theory model over-predicted vertical mixing near elevated sources, but performed much better for ground-level sources. As discussed by [41], the relatively poor behaviour for the elevated source is believed to arise because of a limitation of K-theory models which require the vertical extent of the plume to be comparable to the largest eddy size driving the dilution. This is the reason that the K-theory passive model of Nikmo *et al.* [23] adopts a Gaussian model dispersion model close to the source.

---

[4] *There are some typographic errors in Appendix 6 of* [39]*. We correct these in Appendix B of this report.*

2.3.2 Relative and absolute dispersion

The lateral passive spreading of the plume as specified in [2] is based on the spreading of an instantaneous release [39]. This model is one for so-called relative diffusion, which governs the growth in the relative separation between dispersing particles. This is distinct from absolute diffusion which relates to the observed growth in a fixed frame. Comparison of this spreading rate with the spreading rate from URAHFREP field trial data [17] confirms this, with the predicted spread closely matching the observed 'moving frame' average where the meander of the centroid location has been subtracted.

As discussed by Ott and Jørgensen [42], [17] a model based on relative diffusion has a number of advantages:

- Relative diffusive spread seems to be more amenable to fitting spreading as a universal function of u_* independent of other meteorological parameters *e.g.* stability.
- Plume meander depends on larger scale motions that are more difficult to characterise and scale.
- Inclusion of the effects of plume meander as a dilution can give misleading results, *e.g.* for flammability, for cloud thermodynamics or for buoyancy induced rise.

For determining some hazards, *e.g.* toxic dose at fixed receptor locations, it is desirable to include the effect of plume meander. To compare with measurements from fixed chemical receptors in the URAHFREP field trials, DRIFT was modified to include a 'time averaging' option using an absolute lateral spreading rate due to Draxler and a $t_s^{0.2}$ scaling with averaging time t_s. The minimum spreading, corresponding to a short averaging time, was taken to be the 'instantaneous' value given by the relative diffusion form. For further details reader is referred to [43]. In the absence of a specified averaging time, DRIFT's default is still to use the 'instantaneous' spreading rate corresponding more closely to relative diffusion. A disadvantage of the approach adopted in [43] is that the meander is treated as a dilution potentially affecting the thermodynamic and predicted lift-off behaviour.

Nielsen *et al.* [44] present an alternative meander model, based on modern high quality lidar data, and developed under the EU COFIN Project. Their model has the advantage that it includes asymptotic scaling behaviour that is observed in experiments. However, there is considerable scatter observed between different experiments. This scatter is inherent in the experiments, reflecting non-stationarity of the meander due to changing atmospheric conditions.

2.3.3 Convective boundary layer

In convective atmospheric conditions the cloud may be transported in updraughts or downdraughts. The downward transport of an elevated plume may be greatly enhanced under such conditions. Gaussian passive dispersion models such as ADMS [45] and AERMOD [26] model this using non-Gaussian vertical distributions based on bi-Gaussian PDF models for vertical velocity fluctuations. Including this as additional vertical spread within DRIFT is not straightforward - as for lateral meander there is the danger that the implied dilution will not be appropriate for modelling the thermodynamic behaviour, also integration of the bi-Gaussian distributions with DRIFT's existing profiles is a difficulty. As pointed out by Ott [17], an alternative is to undertake multiple model runs by sampling the vertical velocity w from a suitable probability distribution.

2.4 RECOMMENDATIONS

Based on the above review we make the following recommendations:

- To extend DRIFT's atmospheric profiles to apply also to above the surface layer, but within the mixing layer.
- To include atmospheric temperature and humidity profiles consistent with stability.
- To assume that contaminant is trapped within the mixing layer. This may need to be reviewed for very buoyant releases.
- To base the elevated plume model equations on the models of Ott [17] and Tickle *et al.* [18].
- To aim for a smooth transition between ground based and elevated phases. This would be helped by moving towards a single 'unified' model which evolves between ground-based and elevated phases. It would be advantageous for this to also include the momentum jet phase.
- To model lift-off based on a 'free' buoyant model, accounting for the effect of the ground simply as a truncation of the cloud perimeter.
- To base passive dispersion on relative diffusion (except where specified by K-theory) and to include the effects of meander separately (possibly in post-processing).
- To make a transition from the DRIFT's K-theory passive model for ground-based clouds to a Gaussian passive model for elevated clouds.

The above recommendations are used to guide the model development specified in the subsequent sections of this report.

3 ATMOSPHERE

The atmospheric profiles currently incorporated within DRIFT apply to the lowest 10% of the atmospheric boundary layer (ABL). This lowest layer is called the surface layer (SL). Ground-based dense gas dispersion generally occurs within the SL and in this circumstance adoption of atmospheric profiles based on SL scaling is appropriate. Buoyant clouds, however, may lift from the ground and rise above the surface layer. To cover this circumstance it is necessary to extend DRIFT's atmospheric profile model to be applicable also to the ABL above the surface layer.

The rise of buoyant clouds is influenced by the ambient density profile which is related to the profile of temperature, pressure (and humidity). Humidity also potentially affects cloud buoyancy by virtue of latent heat and heat of mixing. Hence it is necessary to account for the variation of temperature and humidity (and the influence of changing pressure on these).

The following extensions to DRIFT's atmospheric profiles are judged to be necessary:

- Inclusion of profiles of temperature and humidity.
- Extension to include also the ABL region above the surface layer.

The following sections provide a specification of these extensions.

3.1 SCALING REGIONS IN THE ATMOSPHERIC BOUNDARY LAYER

The ABL is modelled using a scaling approach as given in [23]. The boundary layer model assumes horizontal homogeneity. The scaling lengths are the boundary layer height h and the Monin-Obukhov length L_a. The different scaling regions of the ABL are illustrated in Figure 1.

3.1.1 Surface Layer

The surface layer (SL) occupies approximately the lowest 10% of the ABL. In this layer quantities scale according to the height z, the surface stress $\overline{w'u'}_0$ and the surface heat flux $\overline{w'\theta'}_0$. From these the following scaling parameters can be defined for velocity, temperature and length:

$$u_* = \sqrt{\overline{w'u'}_0} \tag{3-1}$$

$$\theta_* = -\overline{w'\theta'}_0 / u_* \tag{3-2}$$

$$L_a = {u_*}^2 \theta_0 / \kappa g \theta_* \tag{3-3}$$

w' is the vertical velocity fluctuation, u' the horizontal along-wind velocity fluctuation and θ' is the potential temperature fluctuation, κ is the von Karman constant, subscript 0 refers to the ground surface value.

3.1.2 Near neutral upper layer

The near neutral upper layer (NNUL) is characterised by the same scaling parameters as the surface layer.

3.1.3 Free convection layer

The free convection layer (FCL) occurs in unstable conditions only and is characterised by the height z and the surface heat flux $\overline{w'\theta'}_0$. The characteristic velocity scale is the free convective velocity

$$w_f = \sqrt[3]{\frac{-\overline{w'\theta'}_0 g z}{\theta_0}} \tag{3-4}$$

3.1.4 Mixed layer

The mixed layer (ML) occurs in unstable conditions only and is characterised by the boundary layer height h and the surface heat flux $\overline{w'\theta'}_0$. The characteristic velocity scale is

$$w_* = \sqrt[3]{\frac{-\overline{w'\theta'}_0 g h}{\theta_0}} \tag{3-5}$$

3.1.5 Entrainment layer

The entrainment layer is influenced by air above the ABL. No scaling parameters are available for this region.

3.1.6 Local scaling layer

The local scaling layer (LSL) occurs in stable conditions only and is characterised by the height z and the *local* stress $\overline{w'u'}$ and *local* heat flux $\overline{w'\theta'}$ resulting in a local characteristic length scale, Λ which may be related to the Monin-Obukhov length L_a [23]

$$\Lambda = L_a \tilde{z}^{\alpha_3} \tag{3-6}$$

$$\tilde{z} = 1 - \frac{z - z_{SL}}{h - z_{SL}} \tag{3-7}$$

with α_3=5/4.

3.1.7 z-less scaling layer

For large values of z/Λ the vertical motions are strongly suppressed and the scaling becomes independent of height z.

3.1.8 Intermittency region

In the intermittency region the turbulence is weak and sporadic; according to [23] no satisfactory theory has been presented for scaling this region.

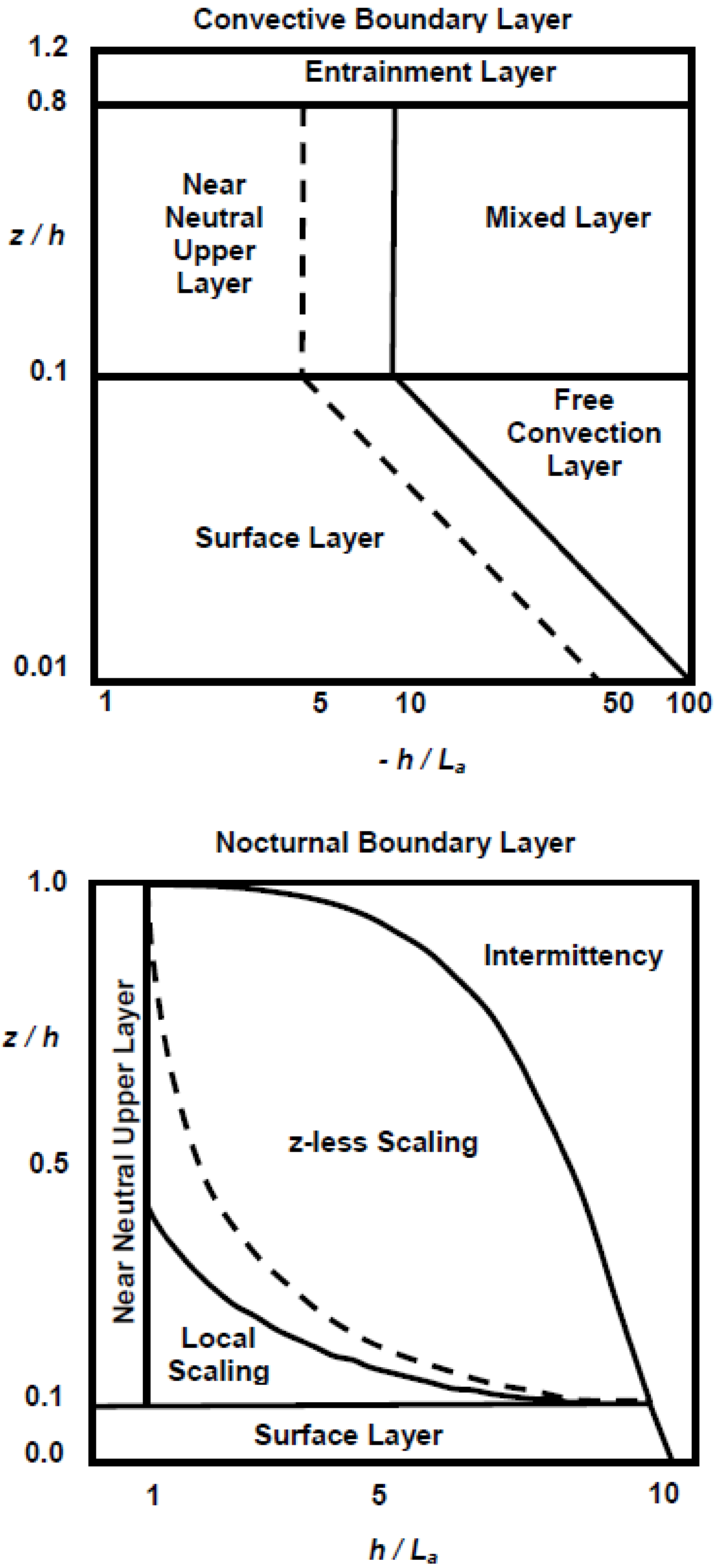

Figure 1 Scaling regions of the ABL

3.2 WIND SPEED AND DIFFUSIVITY PROFILES

3.2.1 Surface layer

The vertical gradient of a mean scalar quantity s is according to Monin-Obukhov similarity theory given by

$$\frac{ds}{dz} = \frac{s_*}{\kappa z}\phi_s(\xi) \tag{3-8}$$

where $s_* = -\overline{w's'}/u_*$ is the scale parameter for the scalar s, ϕ_s is a function of $\xi = z/L_a$.

Integrating (3-8) yields

$$s(z) - s(z_{0s}) = \frac{s_*}{\kappa}\left[\ln\left(\frac{z}{z_{0s}}\right) - \psi_s(\xi) + \psi_s(\xi_{0s})\right] \tag{3-9}$$

where z_{0s} is the lower limit of integration (surface roughness length of scalar s), $\xi_{0s} = z_{0s}/L_a$ and the function ψ_s is given by

$$\psi_s(\xi) = \int_0^{\xi} \frac{1 - \phi_s(\xi')}{\xi'} d\xi' \tag{3-10}$$

The momentum analogue to (3-8) and (3-10) yields the wind speed profile

$$\frac{du_a}{dz} = \frac{u_*}{\kappa z}\phi_m(\xi) \tag{3-11}$$

$$u_a(z) = \frac{u_*}{\kappa}\left[\ln\left(\frac{z}{z_0}\right) - \psi_m\left(\frac{z}{L_a}\right) + \psi_m\left(\frac{z_0}{L_a}\right)\right] \tag{3-12}$$

where z_0 is the surface roughness length.

It is assumed that the transfer of heat and mass are analogous and involve the same transfer functions and roughness lengths, i.e. $\phi_s = \phi_h$ and $z_{0s} = z_{0h}$. However, these are allowed to differ from the momentum transfer functions (see below).

The functions ψ_m, ϕ_m, ψ_h and ϕ_h for the surface layer are are those currently adopted by DRIFT [1], [2], i.e. those of Businger [40] for neutral, stable and unstable with a modification due to Wratt [46] for very stable conditions $z/L_a > 1$.

The vertical diffusivity profile is given by

$$K_z(z) = \frac{\kappa u_* z}{\phi_h(z/L_a)} \tag{3-13}$$

3.2.2 Wind speed above the surface layer

The surface layer profile functions for wind speed may be applied also for $z \gg |L_a|$, possibly even up to $z = h$. For $z > L_a$ the modification due to Wratt [46] is used. It is noted that for the range $1 < z/L_a < 15$ this modified form is numerically similar to the van Ulden and Holtslag function used in [23].

3.2.3 Vertical diffusivity above the surface layer

Nikmo *et al.* [23] give empirical functions for determining the vertical diffusivity above the surface layer. The functions used by [23] are based on the model of Yamartino et al. [47] with slight modifications to remove un-physical discontinuities at the boundaries between the various scaling regions. We follow the same approach, with modifications to account for DRIFT's slightly different surface layer profiles.

3.2.3.1 Near neutral upper layer

The diffusivity in the NNUL is assumed to be constant with height, taking a value equal to K_z at the top of the surface layer.

$$K_z = \frac{\kappa u_* z_{SL}}{\phi_h(z_{SL}/L_a)} \qquad \text{for } 0.1 \le z/h \le 0.8, -10 < h/L_a \le 1. \tag{3-14}$$

A constant diffusivity implies a constant vertical gradient of temperature and humidity.

3.2.3.2 Free convection layer

Following [23] the boundary between the SL and the FCL is defined by $z/L_a = -1$ and

$$K_z = a_1 w_f z \qquad \text{for } z/h \le 0.1, z/L_a < -1. \tag{3-15}$$

where the constant a_1 is determined by requiring continuity of K_z across the SL and FCL boundary.

3.2.3.3 Mixed layer

Following [23] the boundary between the NNUL and the ML is defined by $h/L_a = -10$. The diffusivity is independent of height:

$$K_z = a_2 w_* z_{SL} \qquad \text{for } 0.1 \le z/h \le 0.8, z/L_a < -10. \tag{3-16}$$

where the constant a_2 is determined by requiring continuity of K_z across the FCL and ML boundary $a_2 = (z_{SL}/h)^{1/3}$.

3.2.3.4 Entrainment layer

In the entrainment layer, K_z is assumed to be 10% of the corresponding value in the NNUL or the ML [23].

3.2.3.5 Local scaling layer

The same equations as for the SL are used, except that the surface fluxes are replaced by their local values,

$$K_z = \frac{\kappa\sqrt{\tau}z}{\phi_h(z/\Lambda)} \qquad \text{for } z/h < 1, h/L_a > 1, z/\Lambda \le 1. \tag{3-17}$$

$$\tau = {u_*}^2\tilde{z}^{\alpha_1} \tag{3-18}$$

with $\alpha_1 = 3/2$ and $\tilde{z}$ given by (3-7).

3.2.3.6 z-less scaling layer

The diffusivity in the z-less scaling layer (ZLL) is the asymptotic value of K_z when $z/\Lambda \to 1$

$$K_z = \frac{\kappa\sqrt{\tau}\Lambda}{\phi_h(1)} \qquad \text{for } h/L_a > 1, z/\Lambda > 1, z < z_z. \tag{3-19}$$

where

$$z_z = z_{SL} + (h - z_{SL})\left[1 - \left(\frac{h - z_{SL}}{10L_a}\right)^4\right] \tag{3-20}$$

3.2.3.7 Intermittency layer

In the intermittency layer, K_z is assumed to be 10% of the corresponding value at the top of the underlying layer [23].

3.2.4 Canopy Layer

The wind speed profiles in Section 3.1.1 apply only for heights much greater than the surface roughness length. This was a problem in DRIFT v2 which could not model dispersion of clouds at heights less than twice the roughness length. DRIFT v3 overcomes this problem by modifying the wind speed profile using guidance given in [48] for the wind speed in the canopy layer.

The wind speed, u_a, as a function of height, z, is given by the maximum of the canopy layer wind speed, u_c, and the logarithmic wind speed profile, u_a:

$$u_a(z) = \max[u_c, u_{a1}(z)] \tag{3-21}$$

where $u_{a1}(z)$ is the wind speed profile without the canopy layer modification and the canopy layer wind speed, u_c, is determined from

$$u_c = u_*\left(\frac{z_0}{2H_r}\right)^{-1/2} \tag{3-22}$$

H_r is the average obstacle height in the canopy layer which is set using the simple rule of thumb given in [48]:

$$H_r = 10z_0 \tag{3-23}$$

To maintain correspondence with [1], [2] at heights above the canopy layer, the displacement length d included in [48] is neglected. The advantage of the simplified approach here is that no new inputs are required and correspondence with previous versions of DRIFT is maintained for wind speeds above the canopy layer.

3.3 TURBULENT KINETIC ENERGY DISSIPATION RATE

The elevated passive model requires profiles of the turbulent kinetic energy dissipation rate, ε. The vertical profile of ε is assumed [49] to be

$$\varepsilon = \frac{u_*^3}{\kappa z}\phi_\varepsilon \tag{3-24}$$

with

$$\phi_\varepsilon = \begin{cases} \phi_m - z/L_a & z/L_a \le 0 \\ [1 + 2.5(z/L_a)^{0.6}]^{3/2} & z/L_a > 0 \end{cases} \tag{3-25}$$

Application of (3-25) is most soundly based in the surface layer.

3.4 POTENTIAL TEMPERATURE AND HUMIDITY

The potential temperature θ is defined as the temperature of air when brought adiabatically to a reference pressure. θ is a conserved scalar quantity and, when there is zero heat flux from the ground, θ is constant with height.

The gradient and profile of θ are obtained from (3-9) and (3-11) with the following substitutions:

$$s \to \theta$$

$$s_* \to \theta_* = -\frac{H_0}{\rho_a C_{pa} u_*} = \frac{u_*^2 T_{ref}}{\kappa g L_a}$$

$$z_{0s} \to z_{0h} = z_0 \exp(-\kappa B^{-1})$$

H_0 is the sensible heat flux from the surface, ρ_a is the density of air, C_{pa} is the (mass) specific heat capacity of air, T_{ref} is the reference air temperature used in the definition of the Monin-Obukhov length L_a, B^{-1} is a parameter which is dependent on the terrain. Experiments for homogeneous vegetated surface indicate a value $B^{-1} \approx 6$. More generally, B^{-1} is a function of the roughness Reynolds number $Re_* = u_* z_0/\nu_a$ where ν_a is the molecular (kinematic) viscosity of air (see e.g. [50]).

$\theta_0 = \theta(z_{0h})$ may be determined from the profile function (3-9) together with the potential temperature θ_{ref} corresponding to T_{ref} at the reference height z_{ref}.

Similarly, the specific humidity q_a which is defined as the mass of water per unit mass of moist air is a conserved scalar. The gradient and profile of q_a are obtained from (3-9) and (3-11) with the following substitutions:

$$s \rightarrow q_a$$

$$s_* \rightarrow q_* = -\frac{\lambda E_0}{\rho_a \lambda u_*}$$

$$z_{0s} \rightarrow z_{0q} = z_{0h}$$

λE_0 is the latent heat flux from the surface and λ is the latent heat of vaporisation of water (per unit mass). λE_0 may be determined using the Holtslag weather scheme of DRIFT [51] which is applicable to daytime conditions over a moist grass surface. For the other DRIFT weather schemes λE_0 may be estimated from the surface heat flux H_0 using the Bowen ratio B_o

$$\lambda E_0 = B_o^{-1} H_0 = -B_o^{-1} \rho_a C_{pa} u_* \theta_* \tag{3-26}$$

B_o is dependent upon the nature of the surface [52]. If q and θ are known at two heights then B_o can be determined (see e.g. Panofsky and Dutton [49]). Hanna and Paine [53] indicate that for daytime conditions B_o is positive, with values ranging from 0.1 for water bodies, to 1 for temperate grasslands and as large as 10 for deserts. At nighttime B_0 may take either sign and is difficult to determine by simple weather schemes [54]. In the absence of information on B_o (a candidate for an optional input), it is recommended that $\lambda E_0 = 0$ is assumed, this leads to a constant specific humidity with height.

$q_0 = q_a(z_{0h})$ may be determined from the profile function (3-10) together with the specific humidity $q_{a,ref}$ at the reference height z_{ref}. $q_{a,ref}$ is determined from the input relative humidity $r_{w,ref}$ and temperature T_{ref}:

$$z_{w,ref} = r_{w,ref} \frac{P_{vw}^0(T_{ref})}{P_{ref}}$$

$$q_{a,ref} = \frac{z_{w,ref}}{z_{w,ref}\left(\frac{M_A}{M_w} - 1\right) + 1}$$

where M_A and M_w are the molar masses of dry air and water respectively.

3.5 PRESSURE

The variation of pressure with height is determined from the hydrostatic equation

$$\frac{dP}{dz} = -\rho_a g \tag{3-27}$$

where ρ_a is the density of air and g is the acceleration due to gravity.

3.6 MOIST AIR PROPERTIES

Here we show how the moist air properties are determined from the temperature and water content.

The number of moles of water per mole of moist air, z_w, is determined from the specific humidity q_a

$$z_w = \frac{q_a}{1 + \left(\frac{M_A}{M_w} - 1\right) q_a} \tag{3-28}$$

The relative humidity, r_w is

$$r_w = z_w P / P^0_{vw}(T_a) \tag{3-29}$$

$P^0_{vw}(T_a)$ is the vapour pressure of water at temperature T_a. The air is unsaturated if $z_w < 1$ and saturated if $z_w \geq 1$

$$\left.\begin{aligned} z_{wL} &= 0 \\ z_{wv} &= z_w \end{aligned}\right\} \quad if r_w < 1$$

$$\left.\begin{aligned} z_{wL} &= (r_w - 1)\frac{P^0_{vw}(T_a)}{P - P^0_{vw}(T_a)} \\ z_{wv} &= z_w - z_{wL} \end{aligned}\right\} \quad if r_w \geq 1$$

The molar mass M_a of moist air is

$$M_a = z_A M_A + z_w M_w$$

where $z_A = 1 - z_w$ is the moles of dry air, M_A and M_w are the molar masses of dry air and water respectively.

The molar volume of the moist air is

$$v_a = (z_A + z_{wv})\frac{RT_a}{P} + z_{wL}\frac{M_w}{\rho_{wL}}$$

The moist air density ρ_a is given by

$$\rho_a = M_a / v_a$$

The moist air molar heat capacity C_a is given by

$$C_a = z_A C_A + z_{wv} C_{wv} + z_{wL} C_{wL}$$

where A, wv and wL refer to dry air, water vapour and water liquid values, all evaluated at temperature T_a (and pressure P).

3.7 MIXING HEIGHT

The mixing height, h, (also called the *mixing layer depth* or the *boundary layer depth*) is a measure of the thickness of the ABL and corresponds to a region of enhanced turbulence where atmospheric properties are well mixed. h varies significantly with the diurnal cycle, depending upon the cumulative heat input or loss at the ground and under neutral or stable conditions also the mechanical mixing.

Table 4 of [55] gives typical mixing heights by Pasquill stability category - these values are reproduced in Table 1 of this report.

Table 1 Typical mixing heights [55]

Pasquill stability category	*Typical mixing height (m)*
A	1300
B	900
C	850
D	800
E	400
F	100

Other methods of estimating h are given below.

3.7.1 Neutral conditions

Panofsky and Dutton [49] give

$$h = 0.4\frac{u_*}{f} \tag{3-30}$$

where

$$f = 2\Omega\sin\phi \tag{3-31}$$

is the Coriolis parameter with $\Omega = 7.29\times10^{-5}s^{-1}$ being the Earth's rotation frequency and ϕ the latitude. [49] indicates that in reality h is often smaller than the value given by (3-30) due to large-scale processes leading to elevated inversions capping the turbulent region. Overestimation of h using (3-30) is likely to be greater at larger wind speeds.

3.7.2 Unstable conditions

The growth and decay of the unstable boundary layer during the daytime is dependent upon the energy budget for the layer. Models for h in unstable conditions require detailed information to enable the cumulative effects of heat input and loss to be calculated. The simpler boundary layer height models as in [54] and [26] still need information that is only available in DRIFT's Holtslag weather scheme, taking as input the day of the year, time of day, cloud cover and longitude and latitude.

For the Holtslag scheme the mixing height, h, is calculated using the model of Grying and Batchvarova (1990a) as reported in [56]. The growth of h is determined by

$$\frac{dh}{dt} = \frac{(1+2A)w_*^3 + 2Bu_*^3}{\gamma_\theta \beta h^2} \tag{3-32}$$

where $A = 0.2$ and $B = 2.5$

$$\gamma_\theta \beta = \frac{g}{\theta}\frac{d\theta}{dz} \equiv N_u^2 \tag{3-33}$$

g is the acceleration due to gravity, N_u is the buoyancy frequency which is set equal to the default value of 0.013 [57] and w_* is the convective velocity scale given by equation (3-5).

The transition between mixing height growth in the Convective Boundary Layer according to equation (3-32) and mixing height decay in the Stable Boundary Layer is determined from the point where the net radiative flux at the surface is zero. The net radiative flux at the surface is determined according to the Holtslag method in [51]. The initial value for h in the integration is the equilibrium mixing height in stable conditions (see below).

3.7.3 Stable conditions

Under the Holtslag scheme, the mixing height in stable conditions is calculated following [26]:

$$\frac{dh}{dt} = \frac{h_e - h}{\tau} \tag{3-34}$$

where $\tau = h/(\beta_\tau u_*)$ with $\beta_\tau = 2.0$.

h_e is the equilibrium mixing height calculated using equation A1.1.2a in [56]:

$$\frac{h_e}{L_a} = \left[-1 + \sqrt{1 + \frac{2.28u_*}{|f|L_a}}\right]/3.8 \tag{3-35}$$

which approximates to

$$h/L_a = \frac{0.3u_*/(|f|L_a)}{1 + 1.9h/L_a} \tag{3-36}$$

due to Nieuwstadt.

In the above mixing height calculation $|f|$ is limited by its value at a latitude of 20°.

4 INSTANTANEOUS MODEL

This section presents the extension of DRIFT's instantaneous model equations to include buoyant lift-off and rise.

4.1 THE COORDINATE FRAME

Local Coordinate Frame – Instantaneous Model

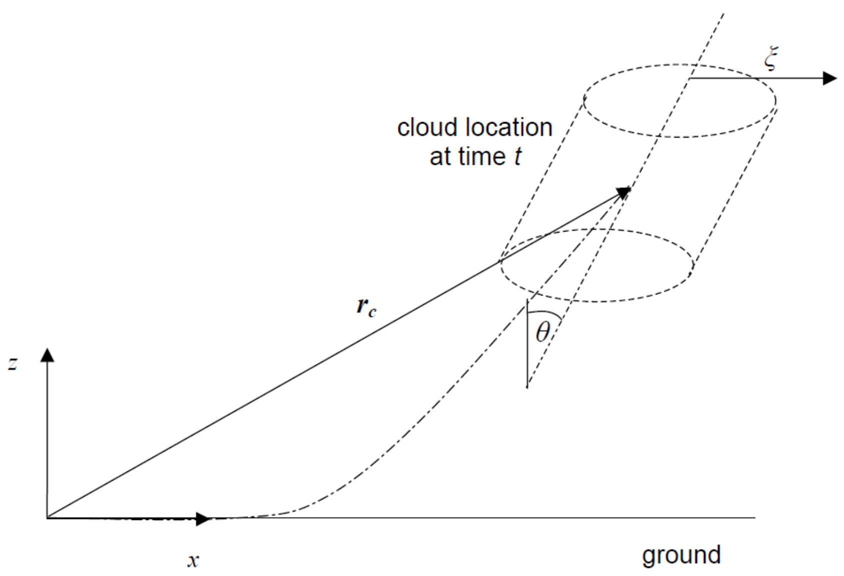

Figure 2 Coordinate Frame for Instantaneous Model

It is necessary to define the coordinate frame for describing the motion and dilution of the cloud. DRIFT [1] defines a Cartesian coordinate system (x, y, z) where x is taken to be in the direction of the wind and z is vertical with $z = 0$ being ground level. In the instantaneous model DRIFT allows the cloud axis to 'lean' due to wind shear. Figure 2 illustrates the coordinate system.

It is convenient to introduce a position vector $\mathbf{r_c} = (x_c, y_c, z_c)$ which points to the cloud centroid location for an elevated cloud, but points to the ground-level cloud centre location for a cloud on the ground.

The unit tangent vector $\hat{\mathbf{e}}_c$ to the trajectory gives the direction of motion of the cloud centroid at a particular time. $\hat{\mathbf{e}}_c = (\cos\theta_c, 0, \sin\theta_c)$ where θ_c is the angle from the horizontal.

For the purpose of defining cloud profiles it is useful to define the relative coordinate ξ

$$\xi = x - x_c - \zeta(z - z_c) \tag{4-1}$$

where ζ is the tangent of the angle between the cloud axis and the vertical.

4.2 CONCENTRATION PROFILES

DRIFT v2 [1] adopts concentration profiles of the form

$$c(x,y,z,t) = C_m(t)F_h(\xi,y)F_v(z)$$

with

$$F_h(0,0) = F_v(0) = 1 \qquad \diamond \tag{4-2}$$

so that C_m is the mean ground-level concentration. The symbol $\diamond$ is used as a reminder that the above equations apply just to the ground-based DRIFT model. We generalise the above to include elevated clouds by defining profiles such that (4-2) is replaced by

$$F_h(0,0) = F_v(z_c) = 1 \tag{4-3}$$

so that C_m is now the mean concentration at location $\mathbf{r_c} = (x_c, y_c = 0, z_c)$.

The horizontal profile F_h is elliptical, given by

$$F_h(\xi,y) = \exp\left[-((\xi/a_1)^2 + (y/a_2)^2)^{w/2}\right] \tag{4-4}$$

where a_1 and a_2 are length scales determining the cloud size in the x and y directions. w is a parameter which determines the sharpness of the edge of the cloud. This is the same form as is used by DRIFT v2 [1]. w is large in the dense gas limit giving a sharp edged cloud and approaches 2 (Gaussian) in the passive limit.

The vertical profile F_v is given by

$$F_v(z) = \tilde{F}_v(z)/\tilde{F}_v(z_c) \tag{4-5}$$

with

$$\tilde{F}_v(z) = s(\hat{z}_c\hat{z})^{(s-1)/2}I_{-\nu}\left(2(\hat{z}\hat{z}_c)^{s/2}\right)\exp(-\hat{z}_c^s - \hat{z}^s) \tag{4-6}$$

$$\hat{z}_c = z_c/a_3 \tag{4-7}$$

$$\hat{z} = z/a_3 \tag{4-8}$$

$$\nu = 1 - 1/s \tag{4-9}$$

a_3 is a length scale determining the vertical extent of the cloud. $I_{-\nu}$ is the modified Bessel function of the first kind of order $-\nu$. The form of F_v is taken from Wheatley's passive puff model for an elevated source [39]. In the limit of a ground-based $z_c \ll a_3$ cloud, F_v reproduces DRIFT's vertical profile as given in [1]. In the limit that $s \to 2$, F_v results in a Gaussian profile with reflection at the ground. For a ground-based ($z_c \ll a_3$) cloud, s will be determined from atmospheric profiles of vertical diffusivity. For an elevated ($z_c \gg a_3$) cloud, we shall require $s \to 2$ so that the cloud profile has a Gaussian shape. Please see Appendix B for further details of Wheatley's model and how it relates to the passive limit of DRIFT.

4.3 CHARACTERISTIC SCALES

Following [1] characteristic cloud lengths may be determined from integrals over the concentration profiles.

The effective cloud height is

$$H = \int_0^h dz\, F_v = a_3/\tilde{F}_v(z_c) \tag{4-10}$$

The effective cloud height H is assumed to be limited by the mixing layer height h.

The cloud centroid height is

$$Z = \frac{1}{H}\int_0^h dz\, zF_v = a_3\widetilde{H}_1 = H/\gamma_0 \tag{4-11}$$

$\widetilde{H}_q$ and γ_0 together with other profile integrals are given Table 2. For the convenience of obtaining simpler closed forms, the integral coefficients in Table 2 are obtained by integration of the profiles from $z = 0$ to $z = \infty$, rather than from $z = 0$ to $z = h$. We interpret this simplification as being broadly equivalent to assuming reflection at the $z = h$ boundary so as to conserve contaminant.

The effective area (horizontal section) is

$$A = \int_{-\infty}^{\infty}\int_{-\infty}^{\infty} d\xi dy F_h \tag{4-12}$$

$$= \pi a_1 a_2 \Gamma(1 + 2/w) \tag{4-13}$$

and effective half-axes are defined by

$$R_1 = a_1\Gamma(1 + 2/w)^{1/2} \tag{4-14}$$
$$R_2 = a_2\Gamma(1 + 2/w)^{1/2} \tag{4-15}$$

so that the area is

$$A = \pi R_1 R_2 \tag{4-16}$$

The perimeter, p_A of the this area is determined as in [1]

$$p_A = 2\pi\sqrt{\frac{R_1^2 + R_2^2}{2}}\, p'_e(\varepsilon) \tag{4-17}$$

where

$$\varepsilon = (R_1^2 - R_2^2)/(R_1^2 + R_2^2) \tag{4-18}$$

and $p'_e(\varepsilon)$ is approximated by

$$p'_e(\varepsilon) = 1 - \left(1 - 2^{3/2}/\pi\right)\varepsilon^2 \tag{4-19}$$

The ground contact area is defined as

$$A_{ground} = F_v(0)A \tag{4-20}$$

and similarly a mixing height contact area is

$$A_h = F_v(h)A \tag{4-21}$$

The quantity

$$f_g = \exp\left[-\left(\frac{z}{2a_3}\right)^2\right] \tag{4-22}$$

provides a useful measure of the degree of grounding, approaching 1 in the limit of a fully grounded ($z_c \ll a_3$) cloud and 0 in the limit of a fully elevated ($z_c \gg a_3$) cloud. The form of f_g chosen here can be thought of as the concentration at the ground from a gaussian concentration distribtution of width $\sim a_3$. Other forms for f_g are possible but we have found that the form given in (4-22) has the desired behaviour and has the advantage of being relatively simple. Similarly, the quantity:

$$f_h = \frac{A_h}{A} \tag{4-23}$$

provides an equivalent measure for the degree of contact between the cloud and the top of the atmospheric boundary layer.

Table 2 Profile integral coefficients

$\widetilde{H}_q = \dfrac{\Gamma((q+1)/s)}{\Gamma(1/s)} M(-q/s, 1/s, -\hat{z}_c^s)$
$\gamma_0 = \left[\widetilde{H}_1 \widetilde{F}_v(\hat{z}_c)\right]^{-1}$
$\gamma_1 = \widetilde{H}_{2-s}/\left[\widetilde{H}_1\right]^{2-s}$
$\gamma_2 = \widetilde{H}_{n+1}/\left[\widetilde{H}_1\right]^{n+1} - \widetilde{H}_n$
$\gamma_3 = \widetilde{H}_2/\left[\widetilde{H}_1\right]^2 - 1$
$\gamma_4 = s\left[\widetilde{H}_1\right]^s$
$\gamma_5 = \lambda(n, s)$
$\lambda(n, s) = \widetilde{H}_n/\left[\widetilde{H}_1\right]^n$
$\widetilde{F}_v(z) = s(\hat{z}_c\hat{z})^{(s-1)/2} I_{-\nu}\left(2(\hat{z}\hat{z}_c)^{s/2}\right)\exp(-\hat{z}_c^s - \hat{z}^s)$
$\nu = 1 - 1/s$
$\hat{z}_c = z_c/a_3$
$\hat{z} = z/a_3$

$M(a, b, z)$ is the confluent hypergeometric function – see e.g. [58]

4.4 DIFFERENTIAL EQUATIONS

The evolution of the instantaneous cloud is governed by a set of ordinary differential equations coupled with a set of algebraic constraints. In general the cloud will contain N_{comp} different substances[5] which are either incondensible or else can condense into one of N_{liq} distinct liquid phases. The equations can be partitioned into those that relate to the bulk motion/composition of the cloud and those that concern its thermodynamic properties. The thermodynamic equations will be dealt with in Section 7 - here we only concern ourselves with those equations specific to the bulk motion/composition. The differential equations are as follows:

[5] *Most often this is air, water and a single contaminant*.

$$\frac{d\Lambda_j}{dt} = f_g U_j^{spread} + Q_\psi \qquad j = 1,2 \tag{4-24}$$

$$\frac{d\zeta\sigma_z}{dt} = Q_\zeta \tag{4-25}$$

$$\frac{dN_i}{dt} = Q_i \tag{4-26}$$

$$\frac{d\mathbf{r}_c}{dt} = \boldsymbol{U} \tag{4-27}$$

$$m\frac{d\mathbf{\Delta U}}{dt} = \widetilde{\boldsymbol{F}} \tag{4-28}$$

$$\frac{ds_c}{dt} = |\boldsymbol{U}| \tag{4-29}$$

$$\frac{d{N_p}^{(drop)}}{dt} = Q_p^{(drop)} \qquad p = 1 \dots N_{liq} \tag{4-30}$$

where t is time and the other symbols will be explained below. The algebraic constraints are given by:

$$V = \pi R_1 R_2 H \tag{4-31}$$

$$s = f_g s_g(Z) + (1 - f_g) s_e \tag{4-32}$$

The thermodynamics provides two extra differential equations and $N_{comp} + N_{liq} + 2$ extra algebraic constraints, but we will postpone discussion of these until Section 7.

The other variables on the left hand side of the differential equations are:

- Λ_j are length parameters related to the effective half-axes, R_j, of the horizontal elliptical cross-section through the cloud, with $j = 1$ corresponding to the downwind direction and $j = 2$ corresponding to the crosswind direction;
- σ_z is the standard deviation of the vertical concentration profile;
- N_i is the number of moles of species i in the cloud;
- m is the mass of the cloud;
- $\boldsymbol{\Delta U}$ is the difference between the cloud velocity and a characteristic velocity $\boldsymbol{U_A}$ related to the wind velocity at the cloud centroid height (see Section 4.7);
- s_c is the distance that the cloud has travelled along its centreline trajectory.
- $N_p^{(drop)}$ is the number of liquid droplets in liquid phase p

The terms on the right hand side of the differential equations determine the evolution of the cloud in time:

- U_j^{spread} are the lateral spreading velocities of the cloud in the downwind ($j = 1$) and crosswind ($j = 2$) directions;
- Q_ψ is a spreading term arising from the derivation of (4-24) from the underlying physics.
- Q_ζ determines the rate of change of the cloud leaning due to shear dispersion in the passive limit. This lean over is suppressed in the dense ground-based dispersion phase;
- $\boldsymbol{U}$ is the cloud velocity;
- $\widetilde{\boldsymbol{F}}$ represents a balance of forces on the cloud that leads to bulk bodily motion.

- Q_i is the rate of change of moles of species i in the cloud. The number of moles may change due to entrainment of ambient fluid (moist air) or deposition of material to the ground;
- U_z is the vertical component of the cloud velocity $\boldsymbol{U}$;
- $Q_p^{(drop)}$ is the rate of change of the number of droplets in liquid phase p;

The variables appearing in the algebraic constraints are:

- $s_g(Z)$ is the ground-based value of s evaluated at the centroid height, Z;
- $s_e = 2$ is the value of s for an elevated cloud.

The above differ from [1] in that the cloud position is now tracked with the vector $\mathbf{r}_c$ and the cloud velocity is now a vector $\boldsymbol{U}$.

4.5 STATIONARY AND NON-STATIONARY INITIAL CLOUDS

For instantaneous releases DRIFT v3 offers the choice of modelling either:

1. A non-stationary initial instantaneous cloud,
2. A stationary initial instantaneous cloud.

These options are described further below.

4.5.1 Non-stationary initial cloud

The non-stationary initial cloud option is the default for instantaneous releases in DRIFT 3.6.7. In this option, the cloud is initialised, not from rest, but with a non-zero lateral spreading velocity and also potentially a non-zero centroid velocity.

This option is intended for scenarios where there has been some initial cloud development prior to the DRIFT instantaneous cloud which can reasonably be judged to give rise to initial cloud expansion and possibly also initial cloud centroid motion. Possible examples are:

- Two-phase flashing releases from catastrophic pressure vessel failure, e.g. as modelled in the source term model ACE [59];
- Instantaneous clouds approximating short duration releases, where there is some prior mixing with air, e.g. vaporisation from a pool, where saturation conditions at the pool surface imply the presence of air, and/or there is time to develop non-zero lateral spreading velocities.

For non-stationary initial clouds, DRIFT calculates the initial centroid velocity based on the amount of air present, the wind speed at the centroid height and an empirical factor that has the effect of slowing the advection speed for dense instantaneous clouds. This empirical factor is described in Section 4.7 .

4.5.2 Stationary initial cloud

The stationary initial cloud option in DRIFT specifies that the cloud centroid and lateral spreading velocities start from zero, irrespective of any initial dilution of the cloud.

This option is intended for scenarios where there is, to a good approximation, no initial motion of the cloud at the point in time when the model source conditions are applied. The lack of initial mixing with air is expected to be rare for accidental instantaneous release scenarios. Possible examples of application of this option are for:

- Thorney Island instantaneous type releases which were released from rest by rapidly removing constraining tent walls.
- Compatibility with DRIFT v2 instantaneous release modelling.

For stationary initial clouds in DRIFT, the gravitational spread of the cloud also includes an empirical delay time which has been found to improve the fit with observations with Thorney Island instantaneous trials. This is the same as the empirical delay time included in DRIFT v2.

4.6 LATERAL SPREADING

The spreading of the horizontal cloud dimensions is modelled according to

$$\frac{d\Lambda_j}{dt} = f_g U_j + Q_\psi \qquad j = 1,2 \tag{4-33}$$

where the Λ_j are related to the R_j via:

$$R_j = \Lambda_j + \frac{4\pi}{9}\left[(1 - f_g)\, a_3 - \Psi z_c\right] \tag{4-34}$$

U_1 and U_2 are velocities appropriate to the lateral spreading of a grounded cloud and Ψ is given by:

$$\Psi = \frac{\sqrt{\pi}}{2} erf\left(\frac{\hat{z}_c}{2}\right) \tag{4-35}$$

and Q_ψ is given by:

$$Q_\psi = \frac{4\pi}{9}\Psi U_z \tag{4-36}$$

The reasoning behind (4-33) is that in the limit $f_g \to 1$ it approaches a ground-based spreading model and in the limit $f_g \to 0$ it approaches an elevated spreading model. Details of these two regimes are expounded below. The Ψ and Q_ψ terms are included to ensure that the spreading is not affected by our particular choice of the form of f_g.

4.6.1 Grounded

For a dilute, neutrally buoyant cloud the grounded spreading velocities, U_i will be determined by passive diffusion; for a sufficiently dense cloud lateral spreading will be determined by gravity spreading.

The lateral spreading velocities are taken to be the maximum of the characteristic gravity spreading and passive spreading velocity scales:

$$U_i = \max\left(U_{i,gravity}, U_{i,passive}\right) \tag{4-37}$$

The gravity spreading velocity is given by

$$U_{1,gravity} = U_{2,gravity} = U_f \quad \text{non-stationary initial cloud} \tag{4-38}$$
$$U_{1,gravity} = U_{2,gravity} = U_f\theta(t - \lambda_g t_G) \text{ stationary initial cloud} \tag{4-39}$$

with U_f is given by

$$U_f = \min\left(K_f(g\Delta' H)^{1/2}, (3g\Delta H)^{1/2}\right) \tag{4-40}$$

where

$$\Delta' = \frac{\rho - \rho_a}{\rho_a} \tag{4-41}$$
$$\Delta = \frac{\rho - \rho_a}{\rho} \tag{4-42}$$

ρ_a is the ambient density at the centroid height. $K_f = 1.07$ is a Froude number constant obtained by fitting against the Thorney Island dense dispersion experiments [3].

The first term in (4-40) represents an approximate balance of forces between gravity driven spreading and air resistance and is found to give a good representation of the dense gas spreading in Thorney Island Trials (after the initial radial acceleration phase). The second term in (4-40) represents a theoretical bound due to the conservation of energy (limiting the kinetic energy of spreading by the initial potential energy). If $\Delta' < 0$, then DRIFT sets $U_f = 0$.

θ in (4-39) is the Heaviside function ($\theta(x) = 1$ for $x > 0$; $\theta(x) = 0$ for $x < 0$). $\lambda_g t_G$ is a characteristic gravity spreading timescale delay which is included to aid comparison with Thorney Island instantaneous release data. This delay is only applied for stationary initial cloud option (see Section 4.5.2).

Passive spreading in the longitudinal (x) direction is determined by

$$U_{1,passive} = \frac{4[\Gamma(1 + 2/w)]^2}{\Gamma(1 + 4/w)} \frac{1}{R_1} \left[\gamma_1 \zeta^2 K_z + 0.3\sigma_{\xi 0}\sigma_u\right] \tag{4-43}$$

and in the lateral (y) direction by

$$U_{2,passive} = \frac{2\Gamma(1 + 2/w)}{\Gamma(1 + 4/w)^{1/2}} 0.3\sigma_v \tag{4-44}$$

where

$$\sigma_{\xi 0} = [\sigma_u/\sigma_v]\sigma_y \tag{4-45}$$
$$\sigma_z = \gamma_3^{1/2} Z \tag{4-46}$$
$$\zeta = \sigma'_z/\sigma_z \tag{4-47}$$

ζ is the tangent of the angle at which the cloud leans over, σ_u and σ_v are the rms ambient velocity fluctuations in the x and y directions which are given by:

$$\sigma_u = 2.5u_* \ , \qquad \sigma_v = 2.0u_* \tag{4-48}$$

The above equations are as given in DRIFT v2 [1], except that the γ_i differ to allow for elevated profiles and are given in Table 2. Also K_z in (4-43) differs, here being interpolated between ground-based K_{zg} and elevated K_{ze} values:

$$K_z = f_g K_{zg} + (1 - f_g) K_{ze} \tag{4-49}$$

The ground-based value K_{zg} is given by the atmospheric diffusivity at the cloud centroid height:

$$K_{zg} = K_z(Z) \tag{4-50}$$

The elevated value K_{ze} is given by

$$K_{ze} = \sigma_z \frac{d\sigma_{ze}}{dt}\bigg|_{passive} \tag{4-51}$$

Here we adopt the passive entrainment model suggested by Ott (equation (137) in [17]), which gives:

$$\frac{d\sigma_{ze}}{dt}\bigg|_{passive} = \frac{1}{\sqrt{2}}\left(\frac{9C\varepsilon\sigma_z}{16}\right)^{1/3} \tag{4-52}$$

with ε being the turbulent kinetic energy dissipation rate at height Z and C is a constant. ε is determined from the atmospheric profiles (see Section 3). Measurements [17] indicate that $C = 0.5$.

4.6.2 Elevated

Buoyant puffs are observed [32] to develop a characteristic flattened spheroidal vortex shape with an up-flow in the centre and the lateral spreading is found to be approximately linear with height. Turner [31] showed that observed vertical rise velocity is consistent with an 'added mass coefficient' for an oblate spheroid with volume $V = 3R^3$ where R is the radius corresponding to the semi-major axis. We shall assume that the aspect ratio implied by this applies to the length scales a_1, a_2 and a_3 giving $a_1 = a_2 = (4\pi/9)a_3$. We may grow from a different aspect ratio cloud towards this by ensuring that

$$\frac{da_1}{dt} = \frac{da_2}{dt} = \frac{4\pi}{9}\frac{da_3}{dt} \tag{4-53}$$

In the elevated limit of $f_g \to 0$ the spreading equations (4-33) are designed to reduce to (4-53)[6].

[6] *This is because the starting point for the derivation of* (4-33) *is a linear interpolation in f_g between the grounded and elevated regimes:*

$$f_g\left(\frac{dR_j}{dt} - U_j\right) + (1 - f_g)\left(\frac{dR_j}{dt} - \frac{4\pi}{9}\frac{da_3}{dt}\right) = 0$$

which eventually gives rise to the Ψ and Q_Ψ terms upon reaching (4-33). *Note that in the elevated limit $R_j = a_j$.*

4.7 CHARACTERISTIC ADVECTION VELOCITY

Improved agreement between predicted instantaneous dense cloud centroid motion and Thorney Island trials is found if the cloud advection speed is reduced below that based on the entrained momentum from the air [60]. To achieve this in DRIFT 3.6.7, a characteristic velocity scale $\boldsymbol{U_A}$ is defined

$$\boldsymbol{U_A} = \left[\lambda_T + \frac{1-\lambda_T}{1+Ri_*}\right]\boldsymbol{U_w} \tag{4-54}$$

where

$$Ri_* = \frac{g\Delta' H}{u_*^2} \tag{4-55}$$

$$\lambda_T = f_g\lambda_{Tg} + \left(1-f_g\right)\lambda_{Te} \tag{4-56}$$

$\boldsymbol{U_w}$ is the wind speed at the cloud centroid height. $\lambda_{Tg} = 0.7$ based on comparisons with experimental data for dense ground-based clouds [60]. $\lambda_{Te} = 1$ to ensure that $\boldsymbol{U_A} = \boldsymbol{U_w}$ so that elevated clouds remain unaffected.

4.8 PROFILE PARAMETERS

The horizontal profile parameter w is given by an interpolation between the ground-based w_g and elevated w_e values

$$w = f_g w_g + (1-f_g)w_e \tag{4-57}$$

where

$$w_g = \begin{cases} 2 + (w_T - 2)(Ri_h/Ri_T) & Ri_h > 0 \\ 2 & Ri_h \le 0 \end{cases} \tag{4-58}$$

with $w_e = 2$ and $w_T = 3$.

Ri_h is a 'horizontal Richardson number':

$$Ri_h = \frac{g\Delta' H}{\sigma_{vc}^2} \tag{4-59}$$

based on the lateral velocity fluctuation

$$\sigma_{vc} = (\sigma_v/u_a(Z))|\boldsymbol{U_h}| \tag{4-60}$$

$$\boldsymbol{U_h} = \boldsymbol{U} - (\boldsymbol{U}\cdot\hat{\mathbf{z}})\hat{\mathbf{z}} \tag{4-61}$$

which is scaled from the ambient lateral fluctuation σ_v. Here, $\hat{\mathbf{z}}$ is a unit vector in the z-direction.

The horizontal profile of the ground-based cloud has a sharp edge for $Ri_h \gg Ri_T$ and tends to a Gaussian as $Ri_h \to 0$ or the cloud becomes buoyant or elevated. The values of Ri_T and w_T are given [43].

The vertical profile parameter s is given by an interpolation between ground-based and elevated values

$$s = f_g s_g + (1 - f_g) s_e \tag{4-62}$$

with the ground-based value being given from the gradient of the atmospheric diffusivity at the centroid height[7]:

$$s_g = 2 - \left.\frac{d\ln(K_{zg})}{d\ln(z)}\right|_{z=Z} \tag{4-63}$$

and the elevated value

$$s_e = 2 \tag{4-64}$$

consistent with a Gaussian profile (constant diffusivity with height).

4.9 WIND SHEAR

The wind shear source term, Q_ζ, in (4-25) is given by:

$$Q_\zeta = \frac{1}{\sigma_z} Q_{\zeta,passive}\, \theta(w_T - w) \tag{4-65}$$

$$\begin{aligned} Q_{\zeta,passive} = {} & \left(\frac{\Gamma(1/s)}{\Gamma(2/s)}\right)^{n+1} (\widetilde{H}_{n+1} - \widetilde{H}_1 \widetilde{H}_n)\, Z U_w(Z) \\ & - \left(\frac{\Gamma(1/s)}{\Gamma(2/s)}\right)^{m} \widetilde{H}_m \zeta K_z(Z) \end{aligned} \tag{4-66}$$

where $U_w(Z)$ is the wind speed at centroid height Z, $m = 2 - s$ and n is given by:

$$n = \left.\frac{dU_w}{dz}\right|_{z=Z} \tag{4-67}$$

As well as inducing a shear transformation to the cloud, the wind shear also provides additional longitudinal dilution, which is encoded in the form of $U_{1,passive}$.

Q_ζ is suppressed for buoyant clouds by multiplying by a smoothed Heaviside function which tends to zero as the Richardson number Ri_* of the cloud becomes large and negative.

4.10 ENTRAINMENT

The volumetric entrainment rate into the cloud is written as:

$$Q = p_A H u_E + A\left(1 - \frac{f_h}{2}\right) u_T \tag{4-68}$$

[7] *This will be modified slightly in Appendix B to smooth out discontinuities between atmospheric layers. See Section B.4 for further details.*

p_A is the perimeter of the ellipse with half axes R_1 and R_2; u_E and u_T are 'edge' and 'top' entrainment velocities. These entrainment velocities are obtained by interpolation between values appropriate for ground-based and elevated clouds:

$$u_E = f_g u_{Eg} + (1 - f_g) u_{Ee} \quad (4\text{-}69)$$
$$u_T = f_g u_{Tg} + (1 - f_g) u_{Te} \quad (4\text{-}70)$$

4.10.1 Grounded

The edge entrainment velocity for the ground-based cloud is given by

$$u_{Eg} = \max\left(u_{Eg,gravity}, u_{E,passive}\right) \quad (4\text{-}71)$$

with the gravity spreading term

$$u_{Eg,gravity} = \alpha_E U_f \quad (4\text{-}72)$$

and $\alpha_E = 0.7$ to optimise fits to Thorney Island data [1].

The top entrainment velocity for the ground-based cloud is

$$u_{Tg} = u_{T,passive} \phi_T(Ri_*) \quad (4\text{-}73)$$

with

$$\phi_T(Ri_*) = \begin{cases} (1 + \lambda_1 Ri_*/Ri_c)^{-1} & Ri_* \geq 0 \\ 1 + \lambda_2 (-Ri_*)^{1/2} & Ri_* < 0 \end{cases} \quad (4\text{-}74)$$

λ_1, λ_2 and Ri_c are constants given in [1], [43].

The passive terms $u_{E,passive}$ and $u_{T,passive}$ are given in Section 4.10.3.

4.10.2 Elevated

In the elevated phase the entrainment velocities are given by

$$u_{Ee} = \max\left(u_{e,buoyancy}, u_{E,passive}\right) \quad (4\text{-}75)$$
$$u_{Te} = u_{T,passive} + u_{e,buoyancy} \quad (4\text{-}76)$$

with

$$u_{e,buoyancy} = \alpha_b |\boldsymbol{\Delta U}| \quad (4\text{-}77)$$

Turner [31] suggests an entrainment coefficient $\alpha_s = 0.23$ for a spheroidal puff. If we were to apply this to an elevated cylindrical cloud with $R_1 = R_2 = 2H$ then

$$\alpha_b = \frac{6}{5}\left(\frac{2}{3}\right)^{1/3} \alpha_s \quad \approx 0.24 \quad (4\text{-}78)$$

The passive terms $u_{E,passive}$ and $u_{T,passive}$ are given in the following section.

4.10.3 Passive

The top entrainment velocity in the passive limit is given by

$$u_{T,passive} = \frac{dH}{dt} = \gamma_4 \gamma_0 K_z / Z \tag{4-79}$$

with K_z given by (4-49) and γ_i given in Table 2.

The edge entrainment velocity in the passive limit is given by

$$u_{E,passive} = \frac{1}{p_A}\frac{dA}{dt} = \frac{\pi}{p_A}\left[R_1 U_{2,passive} + R_2 U_{1,passive}\right] \tag{4-80}$$

with $U_{1,passive}$ and $U_{2,passive}$ given by (4-43) and (4-44).

4.10.4 Initial Dilution with Air

One of the optional inputs to DRIFT is an initial contaminant mass fraction, ϑ_m. Setting this to anything other than unity causes DRIFT to mix an appropriate amount of moist air into the initial cloud. As well as diluting the contaminant, DRIFT's instantaneous model assumes that this initial influx of air brings with it momentum from the atmosphere[8], which yields an initial cloud velocity of:

$$\boldsymbol{U}|_{t=0} = (1 - \vartheta_m)\boldsymbol{U_A} \tag{4-81}$$

Note the use the characteristic velocity $\boldsymbol{U_A}$ here, where $\boldsymbol{U_A}$ is defined in Section 4.7.

4.11 MOMENTUM TRANSFER

The rate of change of excess momentum, $\widetilde{\boldsymbol{F}}$, on the righthand side of (4-28) is given by:

$$\widetilde{\boldsymbol{F}} = \boldsymbol{F} - \boldsymbol{\Delta U}\sum_i M_i Q_i - m\, U_z \frac{d\boldsymbol{U_w}}{dz}\bigg|_{z=Z} \tag{4-82}$$

where Q_i is the rate of change of moles of component i and M_i its molar mass. The reason for expressing the momentum equation in terms of $\boldsymbol{\Delta U}$ instead of $\boldsymbol{U}$ is to minimise subtraction errors in the passive limit[9]. $\boldsymbol{F}$ itself is given by a vector sum of force terms:

$$\boldsymbol{F} = \boldsymbol{F}_{buoyancy} + \boldsymbol{F}_{deposition} + \boldsymbol{F}_{source} + \boldsymbol{F}_{drag} + \boldsymbol{F}_{impact} \tag{4-83}$$

---

[8] *Note that DRIFT does not account for any temperature change caused by mixing in this air; it is assumed that the temperature specified by the user is the temperature after the mixing, not before.*

[9] *Since $\boldsymbol{\Delta U}$ is defined in terms of the characteristic advection velocity scale $\boldsymbol{U_A}$ then strictly the last term in* **Error! Reference source not found.** *should include the gradient of $\boldsymbol{U_A}$, however the Ri* dependence of this makes evaluating this quantity difficult. We therefore simply apply* **Error! Reference source not found.** *as an approximation, noting that this is valid in the passive limit ($Ri_* \to 0$).*

The vertical component of momentum (and hence the vertical component of force) is not modelled for a dense ground-based cloud, i.e. when $\rho > \rho_a$ and $z_c = 0$

$$F_z = 0 \quad (4\text{-}84)$$

$$U_z = 0 \quad (4\text{-}85)$$

Hence, for a ground-based cloud, the vertical momentum is implicit in the centroid motion which is influenced by the combination of gravity spreading and entrainment. Lift-off due to positive buoyancy is incorporated by switching on the buoyancy force when the density $\rho < \rho_a$.

The form of each term is given in the following subsections.

4.11.1 Buoyancy

As already discussed, the vertical forces (the main one being buoyancy) are only modelled when the cloud is elevated $z_c > 0$ or in the case of $z_c = 0$ when the cloud density ρ is less than the ambient density ρ_a at the plume centroid height. The vertical plume buoyancy force is given by

$$\boldsymbol{F}_{buoyancy} = \boldsymbol{g}\frac{(\rho - \rho_a)V}{1 + k_v} \quad (4\text{-}86)$$

The k_v term represents the possibility that not all the buoyant potential energy is transferred to vertical motion of the cloud. This corresponds to the concept of 'virtual' or 'added mass' representing work being done in accelerating ambient fluid which is not directly part of the puff. The added mass coefficient k_v is taken to be that for an oblate spheroid [31]

$$k_v = \frac{\tan\theta_m - \theta_m}{\theta_m - \sin\theta_m \cos\theta_m} \quad (4\text{-}87)$$

where

$$\theta_m = \arccos\left(\frac{a_3}{\sqrt{a_1 a_2}}\right) \quad (4\text{-}88)$$

For $a_3 \geq \sqrt{a_1 a_2}$, the limiting value appropriate for a sphere $k_v = 1/2$ is used.

4.11.2 Deposition

Mass deposition from the puff is assumed to remove momentum corresponding to the deposited material with a characteristic velocity $\boldsymbol{U_{i,D}}$. Accounting for (4-28) being in terms of excess momentum we find

$$\boldsymbol{F}_{deposition} = \sum_i Q_{i,D} M_i (\boldsymbol{U_{i,D}} - \boldsymbol{U}) \quad (4\text{-}89)$$

$Q_{i,D}$ is the molar deposition rate of component i and M_i is the mass per mole. Assuming that the characteristic velocity scale $\boldsymbol{U_{i,D}}$ is equal to that of the plume $\boldsymbol{U_m}$, then (4-89) implies that $\boldsymbol{F}_{deposition} = \boldsymbol{0}$.

4.11.3 Source

In the case of the model calculating dilution (and spreading) over a continuous source, then allowance is made for source material being fed into the puff. Accounting for (4-28) being in terms of excess momentum we find

$$\boldsymbol{F}_{source} = \sum_i Q_{i,S} M_i (\boldsymbol{U_{i,S}} - \boldsymbol{U}) \quad \text{(4-90)}$$

$Q_{i,Q}$ is the molar source rate of component i and M_i is the mass per mole. It is assumed that the characteristic velocity scale $\boldsymbol{U_{i,S}} = \boldsymbol{0}$ for a low momentum source.

4.11.4 Drag

Drag due to friction at the ground is represented by

$$\boldsymbol{F}_{drag} = -\rho u_{*c}^2 A_{ground} \frac{1}{|\boldsymbol{U_w}|^2} [\boldsymbol{U_h}|\boldsymbol{U_h}| - \boldsymbol{U_A}|\boldsymbol{U_A}|] \quad \text{(4-91)}$$

with U_h given by (4-61). Note the use the characteristic velocity $\boldsymbol{U_A}$ here, where $\boldsymbol{U_A}$ is defined in Section 4.7.

The above is a vector form of that given in [1]. However, rather than using u_*, [1] included drag coefficients (β_T and β_E) which were set to zero.

There is no drag contribution for the fully elevated ($A_{ground} \to 0$) puff.

4.11.5 Impact

Following [16], angled impact of an initially elevated cloud is assumed to simply result in deflection of the puff trajectory with no change of speed. This implies an impact force normal to the trajectory:

$$\boldsymbol{F}_{impact} = \begin{cases} \rho U^2 A_{ground} \tan|\theta_c| \boldsymbol{\hat{e}_c} \times \boldsymbol{\hat{y}} & \theta < 0 \\ \boldsymbol{0} & otherwise \end{cases} \quad \text{(4-92)}$$

4.12 HEAT AND MASS TRANSFER TO THE GROUND

DRIFT includes models for heat transfer between the cloud and the ground. Heat transfer may be significant for initially cold clouds moving over a warmer substrate (ground or water).

4.12.1 Heat transfer

The heat flux to the ground is simply modelled as

$$Q_H = A_{ground} S_H \tag{4-93}$$

where S_H is the heat flux per unit area

$$S_H = C_p \rho \langle T'w' \rangle \tag{4-94}$$

which is determined from the maximum of the heat fluxes due to forced and free convection. In the above C_p is the (mass) specific heat capacity of the cloud. In the case that the temperature of the ground is less than the cloud temperature, then the free convection is set to zero. [1] gives details of the determination of the turbulent heat flux term $\langle T'w' \rangle$.

4.12.2 Mass transfer

In additional to heat transfer between the cloud and the ground, DRIFT also offers the option of modelling vapour and liquid deposition. The calculation of mass deposition is optional in DRIFT - the default being that it is disabled.

4.12.3 Vapour deposition

The molar deposition rate $Q_{iv,D}$ of vapour is modelled by analogy with heat transfer

$$Q_{iv,D} = -A_{ground} f_{iv,D} N_{iv} / V \tag{4-95}$$

where f_{iv} is the deposition velocity of component i in the vapour phase, N_{iv} is the number of moles of component i in the vapour phase and V is the total cloud volume. f_{iv} is determined as described in [1].

4.12.4 Liquid deposition

DRIFT's liquid deposition model [1] includes a combination of non-gravitational and gravitational deposition. In the case of a ground-based cloud, transport of liquid through the base of the cloud is reasonably taken to be deposited. For an elevated cloud, the situation is more complex - the non-gravitation deposition term is expected to decrease, whereas gravitational settling may give rise to a 'secondary' puff of lower elevation. For a volatile liquid, even material settling from lower edge of the main cloud may completely vaporise prior to deposition at ground-level. For this reason we choose to model liquid deposition velocity f_{pL} as zero deposition for the elevated plumes. This is obtained by interpolation using the function f_g defined in (4-22):

$$f_{pL} = f_g f_{pL,g} \tag{4-96}$$

where $f_{pL,g}$ is the liquid deposition velocity for the distinct liquid phase p. f_{pL} is calculated as per the ground-based model [1]. The rate of change, $Q_p{}^{(drop)}$ of the number of drops, $N_p{}^{(drop)}$, in each distinct liquid phase p is given by

$$Q_p{}^{(drop)} = -n_p{}^{(drop)} f_{pL} A_{ground} \tag{4-97}$$

where $n_p{}^{(drop)} = N_p{}^{(drop)}/V$ is the number of drops per unit volume in the cloud. The initial value of $N_p{}^{(drop)}$ is calculated from the initial liquid volume of p after flashing and the user input initial mean liquid drop size. Vaporisation of liquid is determined using the homogeneous equilibrium thermodynamic model (see Section 7). The mean size of drops in each liquid phase is calculated from the volume of the liquid phase and the number of drops in that phase. Deposition of liquid drops is neglected for the case where liquid condensation occurs within a gas cloud with initially no aerosol, *e.g.* water mist in a cold cloud.

5 CONTINUOUS MODEL

This section presents the extension of DRIFT's continuous model equations to include momentum, buoyant lift-off and rise.

5.1 UNDEREXPANDED JETS

Extending DRIFT to include momentum jets requires modelling the expansion of the jet from the supplied orifice exit conditions to atmospheric pressure. Releases of superheated liquids - giving rise to flashing two-phase jets, and pressurised gases - giving rise to sonic or subsonic gaseous jets, shall be considered. The region from orifice to atmospheric pressure is bridged by calculating an effective source (pseudo-source in the parlance of Birch *et al.* [61]). Conditions at the orifice are assumed to be known either from a previous calculation, or by direct measurement.

5.1.1 Two-phase flashing jets

We closely follow the approach of Wheatley [62] for the flashing region of the jet. Detailed modelling of the flashing process is not attempted, rather a simple approach is adopted which relates post-flash conditions to those at the orifice by means of a control volume analysis. Various assumptions about the nature of the flow are necessary to close the integral conservation equations.

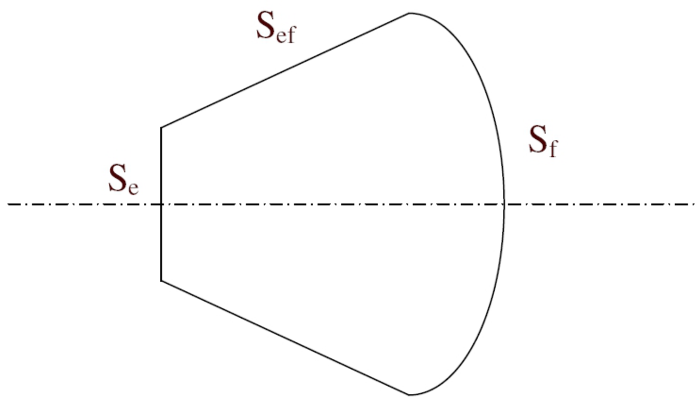

Figure 3 Control volume for flash expansion

The control volume is shown in Figure 3. It is assumed that after flashing the jet has a half-angle θ_f with the flow radial and independent of direction. Conservation equations are obtained by integration over a surface, S, composed of elements S_e, S_{ef}, and S_f. S_e is the exit plane of the orifice of area A_e; S_f is a spherical cap over which it is assumed that the pressure is atmospheric and the two phases are in thermodynamic equilibrium; S_{ef} is the surface of the jet between S_e and S_f defined so that there is no mass, momentum or energy flux across this surface and presumed to be at atmospheric pressure. Such an assumed flow is necessarily a simplification and other assumptions and control volumes are possible. Since the subsequent jet evolution equations neglect the divergence in the flow at S_f, it will be necessary to project quantities onto an equivalent normal plane passing through S_f - this projection is taken as implicit in the following equations.

Mass, momentum and energy conservation for the control volume may be written [62]:

$$q_f = q_e \tag{5-1}$$
$$q_{pf} = q_{pe} + (P_e - P_a)A_e \tag{5-2}$$
$$H_f + \frac{1}{2}\lambda_f^2 U_f^2 = H_e + \frac{1}{2}U_e^2 \tag{5-3}$$

where conditions at the orifice are denoted by subscript e and those after flashing by subscript *f*. q is the mass flux and q_p the momentum flux along the jet axis; H is the specific enthalpy; U the velocity along the jet axis (defined as q_p/q), P_e the exit pressure; P_a the ambient pressure and λ_f is related to the divergence of the jet:

$$\lambda_f = \frac{2}{1 + \cos\theta_f} \tag{5-4}$$

which follows from projection onto the normal plane. Calculation of θ_f would require modelling the radial momentum of the release. This is not done, so θ_f is necessarily an input parameter for the model. In practice it is expected that λ_f will be close to 1.

The above equations assume no entrainment of air and no exchange of heat or momentum through the surface S_{ef} and neglect gravity. Given the flash expansion region is generally short, and in the absence of experimental data to the contrary, these seem reasonable assumptions.

If we further assume a homogeneous mixture, then the specific enthalpy, H of the jet may be written in terms of the liquid and vapour enthalpies and the vapour fraction V:

$$H = H_L + V(H_v - H_L) \tag{5-5}$$

Conditions at the orifice are assumed known. Conditions on S_f (and the normal plane through S_f) correspond, by definition, to equilibrium of the pure contaminant at atmospheric pressure. Hence, given the liquid and vapour enthalpies at the normal boiling point, and since u_f is known from the mass and momentum equations then the final vapour (flash) fraction, x_f may be determined from the energy equation. From x_f and q_f the molar fluxes μ_{gL} and μ_{gv} of released contaminant g can be found.

5.1.2 Gaseous jets

For gaseous releases it is necessary to determine whether the specified release conditions imply the flow is choked (sonic). For choked gaseous flow the conditions after expansion may be determined using the pseudo-source model of Birch *et al.* [61]. For unchoked gaseous flow standard isentropic flow relationships (*e.g.* [63]) may be used to determine the exit conditions from the user input.

5.1.3 A Note on Energy Conservation

The proposed dispersion model balances enthalpy and does not include kinetic energy terms in the energy balance. Therefore, in order to conserve energy from the source, kinetic energy terms must be added at the source. For gaseous releases this amounts to setting the gas temperature equal to the stagnation temperature. For two-phase flashing releases the kinetic energy terms are generally much smaller and are neglected, so that that the energy term in (5-3) becomes:

$$H_f = H_e \tag{5-6}$$

The above assumption essentially means that temperatures predicted and used by DRIFT are stagnation values. Additionally, for the purpose of comparison with experimental data, DRIFT (as of Version 3.7.3) can also output temperature T_{dyn} including cooling based upon the adiabatic relation

$$T_{dyn} = T - \frac{u^2}{2C_p} \tag{5-7}$$

where T is the stagnation temperature, u is the fluid velocity and C_p is the fluid specific heat capacity. DRIFT applies (5-7) to centreline values only.

5.2 THE COORDINATE FRAME

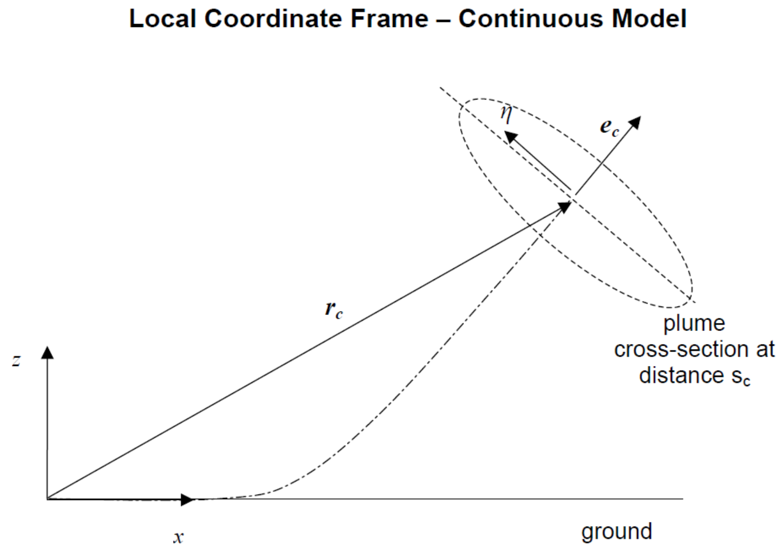

Figure 4 Coordinate Frame for Continuous Model

The steady continuous ground-based plume model in DRIFT v2 defined concentration profiles in the vertical plane at each downwind distance x. Integrating fluxes over the vertical plane yields integral equations where the evolution is in x only. We need to generalise this to the more general case of a plume that is not simply moving horizontally.

A standard approach for elevated plumes is to define a cross-section which is normal to the plume's mean velocity vector and to model the integral fluxes through this cross-section. We choose to follow this. The coordinate system is illustrated Figure 4.

The plume trajectory is described by a vector position $\mathbf{r_c} = (x_c, y_c, z_c)$. As for the instantaneous cloud, $\mathbf{r_c}$ corresponds to the centroid location when the plume is elevated and the ground-level centreline when the plume is on the ground.

s_c is the curvilinear distance along the plume trajectory. Plume integral properties (obtained by integration of profiles over the plume cross-section) evolve as functions of s_c.

The unit tangent vector $\hat{\mathbf{e}}_c$ to the trajectory of $\mathbf{r}_c$ defines the plane of the plume cross-section. $\hat{\mathbf{e}}_\mathbf{c} = (\cos\theta_c \cos\phi_c, \cos\theta_c \sin\phi_c, \sin\theta_c)$ where θ_c is the angle from the horizontal and ϕ_c is the angle from the x-axis.

For the purpose of defining concentration profiles we introduce the orthogonal coordinates ς and η. ς measures distance from the point $\mathbf{r_c}$ along the horizontal line perpendicular to $\hat{\mathbf{e}}_\mathbf{c}$ defined by:

$$\hat{\boldsymbol{\varsigma}} = \frac{\hat{\mathbf{z}} \times \hat{\mathbf{e}}_\mathbf{c}}{|\hat{\mathbf{z}} \times \hat{\mathbf{e}}_\mathbf{c}|} \tag{5-8}$$

η measures distance from the point $\mathbf{r_c}$ along the line whose direction is given by the cross product of $\hat{\mathbf{e}}_\mathbf{c}$ and $\hat{\boldsymbol{\varsigma}}$:

$$\hat{\boldsymbol{\eta}} = \hat{\mathbf{e}}_\mathbf{c} \times \hat{\boldsymbol{\varsigma}} \tag{5-9}$$

A general point (s_c, ς, η) in the plume cross-section can then be expressed as:

$$\boldsymbol{r} = \boldsymbol{r_c}(s_c) + \varsigma \hat{\boldsymbol{\varsigma}}(s_c) + \eta \hat{\boldsymbol{\eta}}(s_c) \tag{5-10}$$

5.3 CONCENTRATION PROFILES

DRIFT's model for ground-based plumes [2] assumes that the steady, time-averaged concentration field has the form

$$c(x, y, z) = C_m(x) F_h(y) F_v(z) \qquad \diamond$$

with

$$F_h(0) = F_v(0) = 1 \qquad \diamond \tag{5-11}$$

so that C_m is the mean ground-level concentration. The symbol ⋄ is used as a reminder that the above equations apply just to the ground-based DRIFT model. We generalise the above to include elevated plumes by writing the concentration as a function of the coordinate s_c and displacements ς and η in the plane of the plume cross-section

$$c(s_c, \varsigma, \eta) = C_m(s_c) F_h(\varsigma) F_\eta(\eta) \tag{5-12}$$

with

$$F_h(0) = F_\eta(0) = 1 \tag{5-13}$$

so that C_m may now be interpreted as the mean concentration at location $\mathbf{r}_c = (x_c, y_c, z_c)$.[10]

The horizontal profile F_h is given by

$$F_h(\varsigma) = \exp[-(\varsigma/b)^w] \tag{5-14}$$

where w is a parameter which determines the sharpness of the edge of the cloud. This is the same form as in DRIFT v2 [2].

The η profile F_η is assumed to have the same profile shape as the instantaneous model (4-5) and is given by

$$F_\eta(\eta) = \tilde{F}_\eta(\eta)/\tilde{F}_\eta(\eta_c) \tag{5-15}$$

with

$$\tilde{F}_\eta(\eta) = s(\hat{\eta}_c\hat{\eta})^{(s-1)/2} I_{-\nu}\left((\hat{\eta}\hat{\eta}_c)^{s/2}\right)\exp(-\hat{\eta}_c^s - \hat{\eta}^s) \tag{5-16}$$

$$\hat{\eta}_c = z_c/a|\cos\theta_c| \tag{5-17}$$

$$\hat{\eta} = \hat{\eta}_c + \eta/a \tag{5-18}$$

$$\nu = 1 - 1/s \tag{5-19}$$

In the limit of a horizontal plume $\theta_c \to 0$ and F_η tends to the elevated passive profile function given in Appendix B . In the limit of a vertical plume $\theta_c \to \pi/2$ and F_η tends to that for an elevated plume with infinite elevation. As long as we ensure that the profile shape parameter s approaches 2 in this limit then this will result in a Gaussian η profile with length scale a. Computer implementation of these profiles requires care to correctly represent these limits whilst avoiding numerical overflows.

5.4 CHARACTERISTIC SCALES

We define characteristic lengths in the η and y directions from integrals of the concentration profile:

$$L_\eta = \int_{\eta_l}^{\eta_u} d\eta\, F_\eta(\eta) = \frac{a}{\tilde{F}_\eta(\hat{\eta}_c)} \tag{5-20}$$

$$L_y = 2W = \int_{-\infty}^{\infty} d\varsigma\, F_h(\varsigma) = 2b\Gamma(1 + 1/w) \tag{5-21}$$

where W is known as the plume half-width. In what follows will occasionally see another parameter, $W_{end-cap}$, and its associated length scale $a_{end-cap}$, appearing in the equations. These quantities relate to the size of the end-caps at the front and back of a finite duration plume. More details of this can be found in Section 6.

The upper and lower limits of the η integral are taken to be

$$\eta_u = (h - z_c)/|\cos\theta_c| \tag{5-22}$$

$$\eta_l = -z_c/|\cos\theta_c| \tag{5-23}$$

[10] *In Section 6 of this report we will formulate a finite duration model of a plume that will have a slightly different concentration profile - for now we proceed under the assumption of a steady continuous plume.*

so that the η extent for an inclined plume is restricted by the ground and mixing layer height. In the limit of a vertical plume the upper and lower limits are $+\infty$ and $-\infty$. As in the instantaneous model case, integral coefficients are obtained by integration of the profiles from $z=0$ to $z=\infty$, rather than from $z=0$ to $z=h$. We interpret this simplification as being broadly equivalent to assuming reflection at the $z=h$ boundary so as to conserve flux.

The effective plume cross-section area is

$$A = L_\eta L_y \tag{5-24}$$

and the vertical extent is

$$H = L_\eta |\cos\theta_c| \tag{5-25}$$

From moments of the concentration profiles

$$\langle\eta^n\rangle = \frac{1}{L_\eta}\int_{\eta_l}^{\eta_u} d\eta\eta^n F_\eta(\eta) \tag{5-26}$$

$$\langle\varsigma^n\rangle = \frac{1}{L_y}\int_{-\infty}^{\infty} d\varsigma\, \varsigma^n F_h(\varsigma) \tag{5-27}$$

we can determine the centroid height

$$Z = z_c + \langle\eta\rangle\cos\theta_c \tag{5-28}$$

and standard deviations of the concentration distribution

$$\sigma_\eta^2 = \langle\eta^2\rangle - \langle\eta\rangle^2 \tag{5-29}$$

$$\sigma_y^2 = \langle\varsigma^2\rangle - \langle\varsigma\rangle^2 \tag{5-30}$$

It is also useful to define a ground contact width

$$L_{ground} = F_\eta(-z_c/|\cos\theta_c|)L_y \tag{5-31}$$

a mixing height contact width

$$L_h = F_\eta((h - z_c)/|\cos\theta|)L_y \tag{5-32}$$

and a free perimeter width

$$L_{free} = 2L_\eta + 2L_y - L_{ground} - L_h \tag{5-33}$$

The quantity

$$f_g = exp\left[-\left(\frac{z_c}{2a\cos\theta_c}\right)^2\right] = e^{-\hat{\eta}_c^2/4} \tag{5-34}$$

provides a useful measure of the degree of plume grounding, approaching 1 in the limit of a fully grounded plume ($\hat{\eta}_c \to 0$) and 0 in the limit of a fully elevated plume ($\hat{\eta}_c \to \infty$). The form of f_g chosen here can be thought of as the concentration at the ground from a gaussian concentration distribution of width $\sim a$. Other forms for f_g are possible but we have found that the form given in (5-34) has the desired behaviour and has the advantage of being relatively simple.

5.5 INTEGRAL FLUXES AND PROFILE FACTORS

The mass flux q_g of contaminant through the plume cross-section is defined by

$$q_g = \int C\boldsymbol{u}(\varsigma,\eta) \cdot \mathbf{d}\boldsymbol{A} \tag{5-35}$$

Writing the plume velocity as the sum of an excess velocity $\boldsymbol{\Delta u}$ and the undisturbed ambient velocity $\boldsymbol{u}_{\mathbf{w}}$:

$$\boldsymbol{u} = \boldsymbol{u}_{\boldsymbol{w}} + \boldsymbol{\Delta u}$$

and substituting into (5-35) gives

$$q_g = C_m A U \tag{5-36}$$

with

$$\boldsymbol{U} = \boldsymbol{U}_w + \boldsymbol{\Delta U} \tag{5-37}$$

$$\boldsymbol{\Delta U} = \frac{1}{A}\int_{-\infty}^{\infty} d\varsigma \int_{\eta_l}^{\eta_u} d\eta\ \boldsymbol{\Delta u} F_h F_\eta \tag{5-38}$$

U is an effective plume velocity, U_w is the wind speed evaluated at the plume centroid height and $\mathbf{\Delta U}$ is an integral measure of the velocity excess.

Hence, following [2] we can define the total mass flux through the plume cross-section

$$q = \rho A U \tag{5-39}$$

where ρ is the density obtained from the plume's effective equation of state as described in [2].

The molar fluxes μ_i follow from the above definitions as described in [2].

We may also define a vector momentum flux for the plume

$$\boldsymbol{q}_p = q\boldsymbol{U} \tag{5-40}$$

The quantities $\mathbf{U}$, q and q_p above are known as *bulk* quantities. It is convenient to assume that the plume excess velocity profile across its cross-section is of the same form as its concentration profile. We can then write $\boldsymbol{\Delta u}(y,\eta) = \boldsymbol{\Delta U_m} F_h(y) F_\eta(\eta)$, where $\boldsymbol{\Delta U_m}$ is the excess *centreline* velocity. In order to be consistent with our definition of q, the excess momentum flux of the cloud is expressed in terms of the excess centreline velocity rather than the excess bulk velocity:

$$\boldsymbol{q}_{pe} = q\boldsymbol{\Delta U_m} \tag{5-41}$$

It is in terms of $\mathbf{q}_{pe}$ that we will express our dynamical equation in section 6. After making the assumption concerning the form of $\boldsymbol{\Delta u}$ we can relate the excess centreline velocity to the excess bulk velocity via:

$$\rho\boldsymbol{\Delta U} = \rho_a(I_1\boldsymbol{U_w} + I_2\boldsymbol{\Delta U_m}) + \Delta\rho\ (I_2\boldsymbol{U_w} + I_3\boldsymbol{\Delta U_m}) \tag{5-42}$$

where the profile factors I_n are given by:

$$I_n = \frac{\Gamma(1/s) + \gamma(1/s, n\hat{\eta}_c^s)}{\Gamma(1/s) + \gamma(1/s, \hat{\eta}_c^s)}\, n^{-1/s-1/w} \tag{5-43}$$

with $\gamma(a, z)$ the lower incomplete gamma function. The profile factors are most relevant to jet releases; however, very close to the jet orifice we assume that the profiles are uniform ($I_n = 1$). This is achieved by instead using a modified set of profile factors, $\tilde{I}_n$:

$$\tilde{I}_n = f_u + (1 - f_u)I_n \tag{5-44}$$

where f_u is a uniform fraction defined by:

$$f_u = \frac{1}{2} erf\left(\frac{\lambda D - s_c}{d}\right) \tag{5-45}$$

where D is the expanded diameter for the jet and s_c the plume coordinate; $\lambda = 7.5$ and $d = 1.5D$. f_u decreases to zero for $s_c \gg 7.5D$. $s_c < 7.5D$ represents the zone of flow establishment for the jet. In general the centreline and bulk velocities will not be parallel[11] and this leads to complications during the derivation of the model. To alleviate these complications we make the further simplification that $\boldsymbol{U}$ and $\boldsymbol{U_m}$ are parallel. To do this we modify the bulk velocity from $\boldsymbol{U}$ to $\widetilde{\boldsymbol{U}}$ to enforce this condition:

$$\boldsymbol{U} \mapsto \widetilde{\boldsymbol{U}} = \frac{U}{U_m}\, \boldsymbol{U_m} \tag{5-46}$$

When solving the differential equations in practice we recover, at each output step, $\boldsymbol{\Delta U_m}$ direct from the solver and then use this to calculate the bulk velocity using (5-42). The corresponding bulk speed is retained but the bulk velocity is then rendered parallel to the centreline velocity using (5-46). Henceforth we drop the tilde from $\widetilde{\mathbf{U}}$ for convenience.

5.6 DIFFERENTIAL EQUATIONS

The evolution of the plume is governed by a set of ordinary differential equations coupled with a set of algebraic constraints. In general the cloud will contain N_{comp} different substances[12] which are either incondensible or else can condense into one of N_{liq} distinct liquid phases. The equations can be partitioned into those that relate to the bulk motion/composition of the cloud and those that concern its thermodynamic properties. The thermodynamic equations will be dealt with in Section 7 - here we only concern ourselves with those equations specific to the bulk motion/composition. The differential equations are as follows:

$$\frac{d\Omega_j}{ds_c} = \beta_j \qquad j = 1,2 \tag{5-47}$$

$$\frac{dt}{ds_c} = U \tag{5-48}$$

---

[11] *Although they often are to a good approximation.*

[12] *Most often this is air, water and a single contaminant.*

$$\frac{d\mu_i}{ds_c} = Q_i \quad (5\text{-}49)$$
$$\frac{d\mathbf{r}_c}{ds_c} = \hat{\boldsymbol{e}}_{\boldsymbol{c}} \quad (5\text{-}50)$$
$$q\frac{d\boldsymbol{\Delta}\mathbf{U_m}}{ds_c} = \widetilde{\boldsymbol{F}} \quad (5\text{-}51)$$
$$\frac{d\mu_p}{dt}^{(drop)} = Q_p^{(drop)} \qquad p = 1 \dots N_{liq} \quad (5\text{-}52)$$
$$\frac{d\zeta\sigma_z}{dt} = f_{passive}Q_\zeta \quad (5\text{-}53)$$
$$q\frac{d\kappa_\updownarrow}{ds_c} = -q'_{entrain}\,\kappa_\updownarrow \quad (5\text{-}54)$$
$$U\frac{dt_\updownarrow}{ds_c} = (1-\kappa_\updownarrow) \quad (5\text{-}55)$$
$$\frac{d\chi_w}{ds_c} = w_{min} \quad (5\text{-}56)$$

where s_c is the plume coordinate. The algebraic constraints are given by:

$$v = L_\eta L_y U \quad (5\text{-}57)$$
$$s = f_g s_g(Z) + (1-f_g)s_e \quad (5\text{-}58)$$
$$U_z = U\sin\theta_c \quad (5\text{-}59)$$
$$W_1 = (1-f_s)\Gamma(1+1/w)a - f_s\Omega_1 \quad (5\text{-}60)$$
$$W_{end-cap} = (1-f_s)\Gamma(1+1/w)a - f_s\Omega_2 \quad (5\text{-}61)$$

There are also two extra differential equations and $N_{comp} + N_{liq} + 2$ extra algebraic constraints arising from the cloud thermodynamics, but we will postpone discussions of these until Section 7.

The variables on the left hand side of the differential equations are:

- Ω_j are length parameters, with Ω_2 related to the plume half-width, W; Ω_1 is related to the plume end-cap radius ($W_{end-cap}$), used primarily in the finite duration model (see below).
- t is the travel time corresponding to s_c;
- μ_i is the molar flux of species i in the plume;
- $\mathbf{r_c}$ is the plume position vector corresponding to s_c as defined in Figure 4;
- q is the mass flux in the plume;
- $\mu_p^{(drop)}$ is the molar flux of liquid droplets in liquid phase p;
- ζ is the tangent of the angle that the cloud centroid axis makes with the vertical[13];
- σ_z is the standard deviation of the vertical concentration profile;
- $\kappa_\updownarrow$, $t_\updownarrow$ and χ_w are used to determine the amount of vertical plume meander in unstable conditions due to updraughts and downdraughts;

[13] *Wind shear was only considered in the instantaneous model in DRIFT v2. In order to match the short-duration limit of a finite duration plume on to an instantaneous puff we now include the effects of wind shear in the continuous model too. More details of this are presented below.*

The terms on the right hand side are:

- β_j is the plume lateral spreading rate in the downwind ($j = 1$) and crosswind ($j = 2$) directions. The downwind spreading rate relates to the end-cap size in the finite duration model (see below);
- Q_i is the rate of change of molar fluxes of species i in the plume;
- $\tilde{\mathbf{F}}$ represents the balance of forces altering the plume momentum;
- $Q_p^{(drop)}$ is the rate of change of the droplet molar flux in liquid phase p;
- Q_ζ determines the rate of change of the cloud leaning due to shear dispersion in the passive limit. This lean over is suppressed in the dense ground-based dispersion phase and in the jet phase - $f_{passive}$ is designed to enforce this latter condition;
- $q'_{entrain}$ is the rate of change of mass entering the cloud due to entrainment;
- w_{min} will be described in Section 5.13.2;

The variables appearing in the algebraic constraints are:

- v is the volume flux in the plume;
- $s_g(Z)$ is the ground-based value of s evaluated at the centroid height, Z;
- $s_e = 2$ is the value of s for an elevated cloud;
- $f_s = f_g^3$ is a smoothing function for transition from axisymmetric spread for the elevated cloud to lateral spreading for the grounded cloud.

The above differential equations are very similar to those in DRIFT v2 [2], except that the momentum flux equation (5-51) is now a vector equation (to allow specification of a vertical component for the elevated plume) and there is now an equation (5-50) to track the position vector $\mathbf{r_c}$.

5.7 LATERAL SPREADING

The spreading of the horizontal dimensions of the ground-level cloud is modelled according to

$$\frac{d\Omega_j}{ds_c} = \beta_j \qquad j = 1,2 \tag{5-62}$$

where the algebraic constraints (5-60) and (5-61) ensure that in the grounded limit $f_s \to 1$ then $W_1 \to \Omega_1$ and $W_{end-cap} \to \Omega_2$. In the limit of an elevated cloud $f_s \to 0$ the algebraic constraints (5-60) and (5-61) ensure that the cloud is axi-symmetric with $W_1 = \Gamma(1 + 1/w)b = \Gamma(1 + 1/w)a$ and $W_{end-cap} = \Gamma(1 + 1/w)a$.

5.7.1 Grounded

The lateral spreading rate β_j of the ground-based plume/jet is based on the model in [19]

$$\beta_j = \max\left(\beta_{jet}, \beta_{gravity}, \beta_{j,passive}\right) \tag{5-63}$$

where

$$\beta_{jet} = f_{jet} \frac{\Gamma(1+1/w)}{(\ln 2)^{1/w}} \frac{dy_{1/2}(jet)}{ds_c} \tag{5-64}$$

is the spreading rate for the ground-based jet. $dy_{1/2}(jet)/ds_c = 0.26$ is the experimentally observed lateral spreading rate for a three-dimensional turbulent jet over a smooth surface as reported by Launder and Rodi [64]. f_{jet} is a function which tends to 1 as the dilution is dominated by jet momentum and zero as the jet dilution term tends to zero (when $\Delta U \to 0$). A function with this behaviour is

$$f_{jet} = \frac{u_{Eg}(jet)(H+W)}{u_{Eg}H + u_{Tg}W} \tag{5-65}$$

where $u_{Eg}(jet)$, u_{Eg} and u_{Tg} are entrainment velocities defined in Section 5.10.1. A further adjustment to f_{jet} is made to account for the observation that the lateral spreading is initially lower close to the source (presumably as result of a region of flow development from the exit conditions to the established wall jet): this is achieved by multiplying f_{jet} by the empirical factor $min(1, 0.38U_0/U_c)$ where U_0 is the initial release speed and U_c is the centreline speed which varies with distance.

The jet spreading rate is further adjusted to avoid excessive (linear) spreading when the jet speed approaches the wind speed by multiplication of β_{jet} by the factor $1 - U_w/(2U)$.

$$\beta_{gravity} = \frac{U_f}{U} \tag{5-66}$$

is the spreading rate due to the gravity spreading velocity U_f acting orthogonally to the edge of the plume[14]. U_f for the continuous plume has the same form as the instantaneous cloud (4-40), except that the Froude number constant K_f differs [4].

The crosswind passive spreading rate $\beta_{2,passive}$ represents the spreading due to ambient turbulence. We write this here as

$$\beta_{2,passive} = u_{E,passive}/U \tag{5-67}$$

where $u_{E,passive}$ is an 'edge' entrainment velocity due to passive diffusion. The form of $u_{E,passive}$ is specified in Section 5.10.3.

The downwind (end-cap) passive spreading rate $\beta_{1,passive}$ is analogous to the downwind spreading rate of the instantaneous model in the passive limit:

$$\beta_{1,passive} = \frac{4\Gamma(1+1/w)\Gamma(1+2/w)}{U\Gamma(1+4/w)} \frac{1}{W_1} \left[\gamma_1 \zeta^2 K_z + 0.3\sigma_{\xi 0}\sigma_u\right] \tag{5-68}$$

---

[14] *This differs slightly from $\beta_{gravity}$ given in* [2], *which has a $\sqrt{U^2 - U_f^2}$ term in the denominator rather than a U. When $U_f \geq U$ a steady plume at the source is not possible without further upwind spread. This will be dealt with in Section 5.14.*

5.7.2 Elevated

The elevated phase is modelled assuming an equal spreading rate of the cross-section length scales a and b (and $a_{end-cap}$):

$$\frac{da}{ds_c} = \frac{db}{ds_c} = \frac{da_{end-cap}}{ds_c} \tag{5-69}$$

which is already encoded in (5-60) and (5-61)(5-62) in the $f_g \to 0$ limit. We can relate $a_{end-cap}$ to $W_{end-cap}$ using:

$$W_{end-cap} = a_{end-cap}\,\Gamma(1 + 1/w) \tag{5-70}$$

which is the direct equivalent of how b is related to W using (5-21).

5.8 PROFILE PARAMETERS

The horizontal and vertical profile parameters w and s are determined exactly as for the instantaneous model (see Section 4.7), except that:

If the release is a moment jet, then f_g in (4-62) is replaced by $f_g f_{passive}$ where $f_{passive}$ is a smoothed heaviside function:

$$f_{passive} = \theta(2 - U/U_w, 0.5) \tag{5-71}$$

defined such that $f_{passive}$ tends to 1.0 in the limit that $U \gg U_w$ and 0 in the limit that U approaches U_w. This changes ensures that the vertical velocity profile is Gaussian for a ground based jet.

The lateral velocity fluctuation appearing in (4-59) is given by

$$\sigma_{vc} = \max\left(\sigma_{v,jet}, \sigma_v\right) \tag{5-72}$$

$$\sigma_{v,jet} = k_{\sigma,jet}|\boldsymbol{\Delta U}| \tag{5-73}$$

rather than (4-60). $k_{\sigma,jet}$ depends upon the lateral distance from the jet centreline. Following EJECT [19], in the absence of data on grounded jets, we estimate $k_{\sigma,jet}$ from data on free circular jets (Rajaratnam [65] Fig. 1.7d) which indicate that typically $k_{\sigma,jet} \sim 0.2$.

5.9 WIND SHEAR

Unlike in [2], we include the effect of wind shear on the concentration profiles in the continuous model. This is done in order to more closely match the short-duration limit of DRIFT's finite duration model on to the instantaneous model (more of which later). The wind shear equation, (5-53), is sourced by Q_ζ, which has the same form as that given in the instantaneous model, (4-65). The lean-over angle affects the concentration profiles by introducing a height-dependent shear to the concentration profiles. This is always along the wind-direction which is not necessarily the direction of travel for the plume. The $f_{passive}$ term in (5-53) is designed to include wind shear effects only when the plume velocity is less than or comparable with the wind speed:

$$f_{passive} = \begin{cases} 1 & U \le U_w \\ \exp\left[-\left(\frac{U - U_w}{U_w}\right)^2\right] & U > U_w \end{cases} \tag{5-74}$$

5.10 ENTRAINMENT

The volumetric entrainment rate of moist air into the plume is written in terms of 'top' and 'edge' entrainment velocities

$$Q = L_y u_T + 2L_\eta u_E \tag{5-75}$$

We note that due to inclination of the plume cross-section 'top' and 'edge' are referred to the length scales L_y and L_η and only have their usual traditional meanings in the limit of a horizontal ground-based plume.

u_T and u_E are obtained by interpolation between values appropriate for ground-based and elevated clouds:

$$u_T = f_g u_{Tg} + (1 - f_g) u_{Te} \tag{5-76}$$
$$u_E = f_g u_{Eg} + (1 - f_g) u_{Ee} \tag{5-77}$$

5.10.1 Grounded

The top entrainment velocity for the ground-based jet/plume is taken to be the maximum of jet and passive terms, modified to account for density stratification in the cloud:

$$u_{Tg} = \max\left[u_{Eg,jet}, u_{T,passive}\right] \phi_T(Ri_*) \tag{5-78}$$

The jet entrainment term is modelled as

$$u_{Eg,jet} = \alpha_{jet} \frac{|\boldsymbol{q_{pe}}|^{1/2}}{\rho_a^{1/2}(W + H)} \tag{5-79}$$

with $\alpha_{jet} = 0.12$. This has the same general form as EJECT's grounded jet model [19], however the value of the entrainment coefficient α_{jet} differs here due to the different definition of velocity profile.

The function ϕ_T is given (4-74). The Richardson number Ri_* needs to account for the turbulent velocity scale $u_{*,jet}$ due to jet shear as well as due ambient shear flow u_*. We therefore replace u_* in (4-55) by u_{*c} as given below:

$$u_{*c} = \max\left(u_{*,jet}, u_*\right) \tag{5-80}$$

where $u_{*,jet}$ is given by

$$u_{*,jet} = \sqrt{C_{jet}{}^{(drag)}}|\mathbf{\Delta U}| \tag{5-81}$$

We assume $C_{jet}{}^{(drag)} = 6.5\times10^{-3}$ taken from EJECT [19] (corrected for the different profiles here) which itself is based on wall shear stress measurements in the centre-plane of bluff wall jets over smooth plates as reported in [65].

The edge entrainment velocity for the ground-based jet/plume is

$$u_{Eg} = \max(u_{Eg,jet}, u_{Eg,gravity}, u_{E,passive}) \tag{5-82}$$

with

$$u_{Eg,gravity} = \alpha_E U_f \tag{5-83}$$

with α_E a constant given in [66]. Equation (5-82) differs from that in DRIFT v2 [2] which uses a variable edge entrainment coefficient to interpolate between the gravity spreading and passive limits. The simpler approach adopted here of taking the maximum is preferred since it uses fewer adjustable parameters.

5.10.2 Elevated

In the elevated phase

$$u_E = u_T = u_e\left(\frac{L_{free}}{2L_\eta + L_y}\right) \tag{5-84}$$

with

$$u_e = f_{e1}\alpha_{e1}|U - U_w\cos\theta| + f_{e2}\alpha_{e2}U_w|\sin\theta| + \alpha_{e3}\left(\varepsilon A^{1/2}\right)^{1/3} \tag{5-85}$$

where α_{e1}, α_{e2} and α_{e3} are constants and ε is the atmospheric kinetic energy dissipation rate (see Section 3.3) which is determined at the centroid height. f_{e1} and f_{e2} are functions which suppress entrainment close to the source. (5-84) is a form that is fairly widely adopted by integral models of elevated plumes and jets in a cross-flow. Appropriate values of the entrainment coefficients α_{e1}, α_{e2} and α_{e3} are dependent upon the assumed plume profiles and whether or not the vertical momentum equation includes added mass (see Section 5.11). Comparison with centreline concentration data for jets in coflow suggest that $\alpha_{e1} = 0.12\sqrt{\pi}/4$ gives good agreement for concentration decay. Comparison with experimental data of buoyant plume lift-off and rise [67] gives best agreement with zero added mass and $\alpha_{e2} = 0.6\sqrt{\pi}/4$. These values are similar to those adopted by EJECT [68] and also Ott [17]. α_{e3} is given by

$$\alpha_{e3} = \left(\frac{9C}{16\sqrt{2\pi}}\right)^{1/3} \tag{5-86}$$

with C = 0.5 [17].

The entrainment suppression terms are based on formulations given in Cleaver and Edwards [69]:

$$f_{1e} = \sqrt{\frac{\bar{\rho}}{\rho_a}} min\left[1, \frac{\mu}{3.7\mu_0}\right]$$

and

$$f_{2e} = \sqrt{\frac{\bar{\rho}}{\rho_a}} min\left[1, max\left[\frac{\frac{s}{L_{se}} - 0.4}{0.6}, 0\right]\right]$$

where μ is the molar flux, μ_0 is the source molar flux, $\bar{\rho}$ is a bulk average density with the approximation

$$\sqrt{\frac{\bar{\rho}}{\rho_a}} = \sqrt{1 + \frac{1}{2}\Delta'}$$

(factor of ½ from integration over profiles). The characteristic length scale L_{se} for suppressing crossflow entrainment is

$$L_{se} = \sqrt{\frac{qU}{\rho_a U_w^2 \pi}}$$

5.10.3 Passive

The top entrainment velocity in the passive limit is given by

$$u_{T,passive} = \frac{dH}{dt} = \gamma_4 \gamma_0 K_z / Z \tag{5-87}$$

with K_z given by (4-49) and γ_i given in 2 with $a_3 = a$.

The edge entrainment velocity in the passive limit is unchanged from [2]

$$u_{E,passive} = 0.3\sigma_v [3\Gamma(1 + 1/w)^3 / \Gamma(1 + 3/w)]^{1/2} \tag{5-88}$$

5.11 MOMENTUM TRANSFER

$\tilde{\mathbf{F}}$ on the righthand side of (5-51) is given by:

$$\widetilde{\boldsymbol{F}} = \boldsymbol{F} - \boldsymbol{\Delta U_m} \sum_i q' - q\,(\hat{\mathbf{e}}_\mathbf{c} \cdot \hat{\mathbf{z}}) \frac{d\mathbf{U_w}}{dz}\bigg|_{z=Z} \tag{5-89}$$

where q' is the rate of change of mass flux in the plume. The reason for expressing the momentum equation in terms of $\mathbf{\Delta U_m}$ instead of $\mathbf{U_m}$ is to minimise subtraction errors. $\mathbf{F}$ is given by a vector sum of force terms:

$$\boldsymbol{F} = \boldsymbol{F}_{buoyancy} + \boldsymbol{F}_{deposition} + \boldsymbol{F}_{drag} + \boldsymbol{F}_{impact} \tag{5-90}$$

The vertical component of momentum (and hence the vertical component of force) is not modelled for a dense ground-based cloud, i.e. when $\rho > \rho_a$ and $z_c = 0$

$$F_z = 0 \tag{5-91}$$
$$U_z = 0 \tag{5-92}$$

Hence for a ground-based plume the vertical momentum is implicit in the centroid motion which is influenced by the combination of gravity spreading and entrainment. Lift-off due to positive buoyancy is incorporated by switching on the buoyancy force when the density $\rho < \rho_a$.

The form of each term is given in the following subsections.

5.11.1 Buoyancy

The vertical buoyancy force is included when the cloud is elevated $z_c > 0$ or in the case of $z_c = 0$ when the cloud density ρ is less than the ambient density ρ_a at the plume centroid height. The vertical plume buoyancy force is given by

$$\boldsymbol{F}_{buoyancy} = \boldsymbol{g}(\rho - \rho_a)A \tag{5-93}$$

Unlike in the instantaneous model we do not include any added mass effects[16].

5.11.2 Deposition

Mass deposition from the plume is assumed to remove momentum corresponding to the deposited material with a characteristic velocity $\boldsymbol{U_{i,D}}$. Accounting for (5-89) being in terms of excess momentum we find

$$\boldsymbol{F}_{deposition} = \sum_i Q_{i,D} M_i \left(\boldsymbol{U_{i,D}} - \boldsymbol{U_m}\right) \tag{5-94}$$

$Q_{i,D}$ is the molar deposition rate of component i and M_i is the mass per mole. Assuming that the characteristic velocity scale $\boldsymbol{U_{i,D}}$ is equal to that of the plume $\boldsymbol{U_m}$, then (5-94) implies that $\boldsymbol{F}_{deposition} = \boldsymbol{0}$.

5.11.3 Drag

Drag due to friction at the ground is represented by

$$\boldsymbol{F}_{drag} = -\rho u_*^2 L_{ground} \frac{1}{|\boldsymbol{U_w}|^2} [\boldsymbol{U_h}|\boldsymbol{U_h}| - \boldsymbol{U_w}|\boldsymbol{U_w}|] \tag{5-95}$$

[16] *The initial specification* [5] *did include an added mass term in the continuous model but comparisons with experimental data in* [67] *were improved when the added mass term was set to zero*

with $\mathbf{U_h}$ defined as in (4-61). This is a vector form of that given in [2]. However, rather than using u_*, [2] included drag coefficients (β_T and β_E) which were set to zero.

There is no drag contribution for the fully elevated ($L_{ground} \to 0$) plume.

5.11.4 Impact

Following [16] angled impact of an initially elevated plume is assumed to simply result in deflection of the trajectory with no change of speed. This implies an impact force normal to the trajectory:

$$\boldsymbol{F}_{impact} = \begin{cases} \rho U^2 L_{ground} \tan|\theta_c| \, \hat{\boldsymbol{\eta}} & \theta < 0 \\ \mathbf{0} & \text{otherwise} \end{cases} \tag{5-96}$$

5.12 HEAT AND MASS TRANSFER TO THE GROUND

DRIFT includes models for heat transfer between the cloud and the ground. Heat transfer may be significant for initially cold clouds moving over a warmer substrate (ground or water). Heat and mass transfer modelling for DRIFT's continuous model is directly analogous to the instantaneous model, with A_{ground} in the instantaneous model being replaced by L_{ground}.

5.13 PLUME MEANDER

5.13.1 Lateral

We account for lateral plume meander in post-processing (after the model has run) by adjusting the value of the lateral spread parameter $b \equiv b(0) \mapsto b(t_s)$ in the concentration profiles, where t_s is the user input averaging time. We characterise the width of the horizontal concentration profile in terms of a parameter σ_y, which is related to b via:

$$\left(\frac{\sigma_y}{b}\right)^2 = \frac{\Gamma(3/w)}{\Gamma(1/w)} \tag{5-97}$$

In the passive limit $\sigma_y(0)$ reduces to $\sigma_{y,passive}(0)$, which is assumed to take the following form [42]:

$$\sigma_{y,passive}(0) = 0.8 u_* t \tag{5-98}$$

where t is the travel time along the plume trajectory. The effect of lateral meander is to modify $\sigma_{y,passive}(0)$ to $\sigma_{y,passive}(t_s)$, which is given by:

$$\sigma_{y,passive}^2(t_s) - \sigma_{y,passive}^2(0) = \frac{\lambda \sigma_{y,passive}(0) U_w T^3}{t_s^2}\left(1 - t_s/T + \frac{1}{2}(t_s/T)^2 - e^{-t_s/T}\right) \tag{5-99}$$

with $\lambda = 0.2$ and $T = 30\sigma_{y,passive}(0)/U_w$ [44]. Assuming that the change in $\sigma_{y,passive}$ equates to an equivalent change of the overall σ_y, we can write:

$$\sigma_y^2(t_s) - \sigma_y^2(0) = \frac{\lambda \sigma_{y,passive}(0) U_w T^3}{t_s^2}\left(1 - t_s/T + \frac{1}{2}(t_s/T)^2 - e^{-t_s/T}\right) \tag{5-100}$$

5.13.2 Vertical

The vertical plume meander reflects the deviation of the plume due to updraughts and downdraughts, which are stochastic in nature and are assumed to occur in unstable conditions only. One way to do this is to undertake multiple runs sampling from a suitable probability distribution. However, this is potentially very time-intensive, and so an alternative approach is employed based on a very simple one-dimensional model. Given an updraught (or downdraught[17]) of constant velocity w we can write the following equation for vertical momentum conservation in the plume[18]:

$$\frac{d(qv)}{ds_c} = w q_{entrain}' \tag{5-101}$$

where v is the cloud vertical velocity and q is the mass flux. This can be rearranged to give:

$$\frac{1}{w-v}\frac{dv}{ds_c} = \frac{q_{entrain}'}{q} = -\frac{d\ln\kappa_\updownarrow}{ds_c} \tag{5-102}$$

which serves as the definition for a new variable, $\kappa_\updownarrow$, which yields (5-54), repeated here for clarity:

$$q\frac{d\kappa_\updownarrow}{ds_c} = -q_{entrain}'\,\kappa_\updownarrow$$

We are now in a position to estimate the vertical displacement, $z_\updownarrow$ of the cloud due to the air entrainment, defined by:

$$\frac{dz_\updownarrow}{dt} = v \tag{5-103}$$

Integrating (5-102) yields:

[17] *We consider downdraughts to be up-draughts with negative velocity.*
[18] *For simplicity we assume that the only mechanism acting to perturb the vertical motion of the cloud is entrainment of air from the atmosphere.*

$$\int \frac{dv}{w-v} = -\ln\left(\frac{w-v}{w}\right) = -\ln\kappa_{\updownarrow} \tag{5-104}$$

which uses the condition that the initial vertical velocity perturbation of the plume is zero. This leads to:

$$\frac{dz_{\updownarrow}}{dt} = w(1-\kappa_{\updownarrow}) \tag{5-105}$$

We next define a meander time, $t_{\updownarrow}$, via:

$$z_{\updownarrow} = wt_{\updownarrow} \tag{5-106}$$

and use the fact that $d/dt = Ud/ds_c$ to reach the following equation, which is independent of w:

$$U\frac{dt_{\updownarrow}}{ds_c} = (1-\kappa_{\updownarrow}) \tag{5-107}$$

Note that exactly the same set of equations can be obtained by considering the effects of updraughts and downdraughts as a small perturbation to the momentum equation (5-51).[19] We now assume that the probability density of a particular updraught strength, w, is given by $p(w)$. Given the form of $p(w)$ and assuming that $z_{\updownarrow}$ acts to adjust the cloud height, z_c, we can take the effects of vertical meander into account by calculating a modified vertical concentration distribution, $\tilde{F}_{\eta\updownarrow}(s_c,\eta)$, from the unmodified vertical distribution $\tilde{F}_{\eta}(s_c,\eta;\ \ z_c)$, with cloud height z_c, as follows:

$$\tilde{F}_{\eta\updownarrow}(s_c,\eta) = \int_{-\infty}^{\infty} dw\ \ p(w)\,\tilde{F}_{\eta}(s_c,\eta;\ \ \max(z_c + wt_{\updownarrow}, 0)) \tag{5-108}$$

where z_c and $t_{\updownarrow}$ are implicitly functions of s_c. The $\max(z_c + wt_{\updownarrow}, 0)$ in this equation reflects the fact that the maximum effect a downdraught can have is to bring the cloud down to the ground.

However, (5-108) strictly applies for an elevated plume only where the vertical forces acting on the bulk motion of the cloud are taken into account in (5-54). In the case of a grounded dense (or passive) plume our model assumes that the cloud remains fixed at $z_c = 0$. In this regime downdraughts are assumed to play no role in the centreline motion and updraughts are suppressed by the buoyancy of a dense cloud. Returning to the momentum equation (5-101) we can estimate the minimum velocity, ${w_{min}}^{(g)}$, that an updraught needs to overcome the cloud buoyancy force and enable a dense plume to lift off the ground:

$${w_{min}}^{(\mathrm{g})} = -\frac{\boldsymbol{F}_{buoyancy}\cdot\hat{\mathbf{z}}}{{q_{\mathrm{entrain}}}'} \tag{5-109}$$

If we compute the mean value, ${\bar{w}_{min}}^{(g)}$, of ${w_{min}}^{(g)}$ as the plume progresses then we can roughly account for the effects of updraught suppression by modifying (5-108) to:

---

[19] *This is achieved by making the substitutions $\boldsymbol{\Delta U_m} \mapsto \boldsymbol{\Delta U_m} + w\alpha\hat{\mathbf{z}}$ and $\boldsymbol{F} \mapsto \boldsymbol{F} + w{q_{entrain}}'\,\hat{\mathbf{z}}$ where $\alpha = 1-\kappa_{\updownarrow}$. Collecting together the w terms in the equation leads to* (5-54).

$$\tilde{F}_{\eta\updownarrow}(s_c,\eta) = \int_{-\infty}^{\infty} dw\;\; p(w)\; \tilde{F}_\eta(s_c,\eta;\;\; \max((w - \overline{w}_{min}{}^{(g)})t_\updownarrow, 0)) \tag{5-110}$$

which holds exactly in the case that $w_{min}{}^{(g)}$ is a constant. In the case of a plume that lifts-off or touches-down over the course of its trajectory it is less clear how to proceed. In order not to over-complicate matters we adopt the following general form for $c_\updownarrow$:

$$\tilde{F}_{\eta\updownarrow}(s_c,\eta) = \int_{-\infty}^{\infty} dw\;\; p(w)\; \tilde{F}_\eta(s_c,\eta;\;\; \max(z_c + (w - \overline{w}_{min})t_\updownarrow, 0)) \tag{5-111}$$

where $\overline{w}_{min}$ can be calculated using the following differential equation:

$$\frac{d\chi_w}{ds_c} = w_{min} \qquad \text{where} \qquad \chi_w = s_c\overline{w}_{min} \tag{5-112}$$

with

$$w_{min} = \begin{cases} w_{min}{}^{(g)} & \text{grounded} \\ 0 & \text{elevated} \end{cases} \tag{5-113}$$

We recognise that Equation (5-111) is a simplification, but it has the merit of tending to (5-108) and (5-110) in the fully elevated and fully grounded limits respectively.

It remains to give the details of $p(w)$ itself. In DRIFT we assume that w is distributed according to the sum of two Gaussians, as presented by Weil *et al.* [69]:

$$p(w) = \sum_{i=1}^{2} \frac{\lambda_i}{\sqrt{2\pi}\sigma_{wi}} \exp\left[-\frac{(w-\overline{w_i})^2}{2\sigma_{wi}^2}\right] \tag{5-114}$$

with

$$\frac{\overline{w_1}}{\sigma_w} = \frac{\gamma_1 S}{2} + \frac{1}{2}\left(\gamma_1^2 S^2 + \frac{4}{\gamma_2}\right)^{1/2} \tag{5-115}$$

$$\frac{\overline{w_2}}{\sigma_w} = \frac{\gamma_1 S}{2} - \frac{1}{2}\left(\gamma_1^2 S^2 + \frac{4}{\gamma_2}\right)^{1/2} \tag{5-116}$$

where

$$\gamma_1 = \frac{1+R^2}{1+3R^2} \tag{5-117}$$

and

$$\gamma_2 = 1 + R^2 \tag{5-118}$$

The λ_i are given by:

$$\lambda_1 = \frac{\overline{w_2}}{\overline{w_2} - \overline{w_1}} \tag{5-119}$$

$$\lambda_2 = -\frac{\overline{w_1}}{\overline{w_2} - \overline{w_1}} \tag{5-120}$$

$R = 2$, $\sigma_{w1} = R\,\overline{w_1}$ and $\sigma_{w2} = -R\,\overline{w_2}$. The skewness $S = \overline{w^3}/\sigma_w^3$ is parameterised by:

$$S = 0.105\left(\frac{w_*}{\sigma_w}\right)^3 \tag{5-121}$$

σ_w in the Convective Boundary Layer (CBL) is parameterised by

$$\sigma_w^2 = 3.6u_*^2 + 0.31w_*^2 \tag{5-122}$$

5.14 UPWIND SPREAD AND PLUME INITIALISATION

DRIFT v2 assumes that the material evolved from an area source (usually thought of as a pool) exits horizontally through a *vertical source window* of a user specified width. Usually the source window width is selected to match the width of the source. One of the limitations of DRIFT v2 is when the gravity spreading velocity, U_f, at the source becomes large compared with the plume speed U.

In DRIFT v2 the plume gravity spreading rate, $\beta_{gravity}$, is given by

$$\beta_{gravity} = \frac{U_f}{\sqrt{U^2 - U_f^2}} \tag{5-123}$$

which is undefined when $U \leq U_f$, indicating that a steady plume cannot exist with the specified conditions. Rather, the material from the source would be expected to spread upwind until it reaches a size such that $U > U_f$ in which case a steady gravity spreading plume solution is possible. Whereas DRIFT v2 required manual adjustment of the source to overcome this problem, DRIFT v3 incorporates a new sub-model to deal specifically with this. This upwind spreading model is described below.

The continuous model in DRIFT v3 has two distinct initialisation regimes: momentum jets and low momentum area sources. The former have already been dealt with in section 1. The low momentum area source case concerns us here[20].

The low momentum area source is circular of a user-specified size[21]. For dense and passive releases we wish to calculate a steady source window from which to evolve the plume. To do this DRIFT will initially run its ‘instantaneous’ model beginning with an infinitessimally thin cylinder of material completely covering the source. Unlike in the standard instantaneous model we assume material is fed into the cloud at a steady rate equal to the source release rate[22] and allow the model to run until the following conditions, designed to ensure that the resultant source window is consistent with a steady plume:

- The downwind spreading velocity, U_1, must be less than the windspeed, U_w;
- The initial bulk speed, U, of the resultant plume must satisfy $U < U_w + U_1$.

[20] *When running DRIFT v3 for a low momentum area source the user can choose whether to calculate initial dilution over the source, which is the default scenario described in this section. However, if this option is deselected then DRIFT v3 will initialise the plume through a source window analogous to the initialisation procedure in DRIFT v2.*
[21] *More generally this can be an elliptical pool.*
[22] *For simplicity we neglect ground transfer and cloud tilt in this procedure.*

When these conditions are met DRIFT performs a transition to a steady continuous model with an effective source window of half-width $W^{(cont)} = R_2^{(inst)}$ and height $H^{(cont)} = H^{(inst)}$ with modified release rate and composition due to the entrainment of moist air during the instantaneous model expansion. During the instantaneous model phase DRIFT allows the cloud centroid to move downstream (based on the air entrainment) provided that the cloud back-end does not cross the upwind edge of the source. The effective source window may therefore be downstream of the initial source location.

In DRIFT v3 the spreading equation (5-123) is replaced by (5-66). This simplification is justified on the basis that the main effect of (5-123) is included by using the instantaneous model to determine upwind spreading at the source, and that subsequently, when $U > U_f$, (5-66) is a good approximation of (5-123).

Using the above method it is possible that the instantaneous model phase of the DRIFT run will fall below the concentration/dose levels of interest before a steady source window can be established. In this case, a transient calculation can be performed using DRIFT's finite duration model (see Section 6).

In DRIFT the numerical value of the frontal Froude number K_f differs between the instantaneous and continuous models, with a lower value of 0.4 being adopted for the continuous model as compared with 1.07 for the instantaneous model. The upwind spreading calculation described above for continuous releases uses the continuous model Froude number - this gives smoother behaviour for short duration releases modelled using DRIFT's finite duration model.

In the case of very buoyant material evolving from a pool DRIFT does not adopt the above approach, but instead models the release as an initially vertically-oriented buoyant plume. Low momentum, slightly buoyant releases can experience very strong bending of the plume trajectory which can lead to numerical difficulties for the solver used by DRIFT v3 - in this circumstance feeding the buoyant material into an initial instantaneous cloud and then transitioning to a steady release through a vertical source window is found to improve numerical stability. The following criterion is found to work reasonably well and give reasonable behaviour compared with buoyant plume wind-tunnel data [67]: for $U < 2.5\,U_w$ an upfront instantaneous model run is used; all other low momentum buoyant releases are modelled as initially vertically-oriented buoyant plumes.

6 FINITE DURATION AND TIME-VARYING RELEASES IN DRIFT

In the previous sections we have presented two models: the first is the model of an instantaneous release of a fixed amount of material; the second is a model of a steady continuous release of material that continues for an infinite amount of time. In this section we extend DRIFT to deal with finite duration and time-varying releases. We deal with the finite duration case first.

6.1 FINITE DURATION RELEASES

In the finite duration model we assume that the release of material continues at a constant release rate, $\dot{m}$, for a fixed amount of time, t_{rel}, and then terminates abruptly. The basic equations are the same as in the steady continuous model except that we now treat the cloud differently in post-processing.

In the steady continuous model we can associate a travel time, t, with a given cross-section through the cloud perpendicular to its direction of travel. Given the release start time and the release end time we can identify cross-sections through the plume that are associated with the front, $s_f(t)$, and back, $s_b(t)$, of the cloud at any given time. Whilst the release is still ongoing the back of the cloud will always be at the source but the front will move progressively further downstream; once the release has terminated the back of the cloud will begin to move off downstream as well.

As time progresses the ends of the plume (referred to here as end-caps) will grow and, in addition to lateral mixing, there is also longitudinal mixing across the ends. Long after the release has ceased, the size of the two end-caps will be large compared to the separation between them and in this limit the cloud will start to look like a cloud resulting from an instantaneous release. Conversely, in the limit $t_{rel} \to \infty$ the front end-cap will move infinitely far downstream whilst the back end-cap remains at the source and the cloud will grow to look like that from a steady continuous release.

In the equations of Section 5 we have seen how the equation for the end-cap size, $W_{end-cap}$, has been included in the continuous model, based on the formalism of the instantaneous model. This introduces a parameter $a_{end-cap}$ representing the profile length scale in the longitudinal direction near to this end-cap. In order to account for the mixing of the material across the front and back of the clouds we modify the centreline concentration, $C_m(s_c)$, calculated in the pure continuous model, to give a time-dependent concentration, $C(s_c, t)$ based on the positions of the front and back end-caps with time.

To develop the approach, we examine the effect of mixing across an end-cap on a simple concentration profile. We define a function $P(s, s_f, s_b)$ of the front and back locations s_f and s_b at time t such that

$$C(s_c, t) = C_m(s_c)P(s_c, s_f(t), s_b(t)). \qquad (6\text{-}1)$$

In the case of an idealised finite duration release ignoring longitudinal mixing at the front and back of the cloud then

$$P(s, s_f, s_b) = P_0(s, s_f, s_b) \equiv \theta(s_f - s) - \theta(s_b - s). \tag{6-2}$$

where $\theta(s)$ is the Heaviside function defined by

$$\theta(s) = \begin{cases} 1, & s \geq 0 \\ 0 & \text{otherwise} \end{cases} \tag{6-3}$$

The Heaviside function in (6-2) is too sharp to represent the ends of a real cloud: a smoother representation for $P(s, s_f, s_b)$ can be obtained by convoluting $P_0(s, s_f, s_b)$ with a normalised instantaneous cloud profile shape, $\mathcal{J}(s_c)$, given by:

$$\mathcal{J}(s) = \frac{\Gamma(1/w)}{\pi\, a\, \Gamma(2/w)} \exp\left[-\left\{\left(\frac{s}{a}\right)^2 + \left(\frac{\varsigma}{b}\right)^2\right\}^{w/2}\right] \tag{6-4}$$

where a is the end-cap characteristic length scale and w is the profile sharpness parameter. The convolution is defined by

$$P(s_c, s_f, s_b) \equiv \int_{s_b}^{s_f} ds \mathcal{J}(s_c - s) \tag{6-5}$$

The reason that a convolution is chosen for smearing the front and back ends of the finite duration cloud rather than some other smooth function is that a convolution has the following useful properties:

- it is inherently mass preserving when $\mathcal{J}(s)$ is normalised;
- it 'erodes' the central steady plume proportion as the end-cap length scale a grows;
- in the limit that $(s_f - s_b)/a \to 0$ (6-5) corresponds to an instantaneous puff with profiles described by (6-4);
- it has the following additive property that is useful for adding adjacent finite duration cloud segments when we consider the time-varying model:

$$P(s_c, s_1, s_2) + P(s_c, s_2, s_3) = P(s_c, s_1, s_3) \tag{6-6}$$

In general the end cap parameters a, b and w will differ between the front and back ends of the cloud. We account for this variation approximately by evaluating $P(s_c, s_f, s_b)$ separately for the front and back of the cloud using fixed front and back end cap parameters for each (denoted by P_f and P_b respectively)[23]. DRIFT determines P_f and P_b by numerically integrating (6-5). The profiles for the different parts of the cloud are then combined using the following interpolation procedure:

$$\begin{aligned} C(s_c, t) = \lambda_b C_m(s_b(t)) P_b\big(s_c, s_f(t), s_b(t)\big) + \lambda_c C_m(s_c) F_h(\varsigma) \\ + \lambda_f C_m(s_f(t)) P_f\big(s_c, s_f(t), s_b(t)\big) \end{aligned} \tag{6-7}$$

where

$$\lambda_f = \begin{cases} e^{-\mu(s_f - s_c)/a(s_f)} & s_c < s_f \\ 1 & \text{otherwise} \end{cases} \tag{6-8}$$

$$\lambda_b = \begin{cases} e^{-\mu(s_c - s_b)/a(s_b)} & s_c > s_b \\ 1 & \text{otherwise} \end{cases} \tag{6-9}$$

$$\lambda_c = \max(0, 1 - \lambda_f - \lambda_b) \tag{6-10}$$

[23] *This corresponds to assuming that the parameters change slowly over the distance scale a*

with $\mu = 2$ chosen to smoothly approach the steady continuous solution sufficiently far from the end caps.

Whilst the release is active, the back-end of the cloud is held fixed at $s_b = 0$, with the back-end profile parameters determined from the steady source conditions (including upwind spread and a delay to establish the steady source where appropriate[24]). When the release stops, s_b moves downstream as determined by the plume travel distance with time. For a maintained release (as $t \to \infty$) (6-7) recovers the steady plume limit with $s_b = 0$ and $s_f \to \infty$.

The time averaging for the finite duration model is as described in Section 5.13, with maximum time for averaging being limited by the release duration.

The above forms the basis of the finite duration model in DRIFT. This approach ensures:

- long after the release has ceased, the concentration profiles tend to those of the instantaneous model;
- in the limit of a long release time compared with the cloud travel time, the concentration profiles tend to those of the steady continuous model;
- the model gives smooth behaviour between these limits.

Similar approaches, sometimes using the language of travelling observers, for finite duration and time-varying releases has been adopted by other published integral models (e.g. HGSYSTEM [16], UDM [22], SLAB [70] and ADMS [45]).

6.2 TIME-VARYING RELEASES

DRIFT's time-varying model is based upon splitting a time-varying release into a series of finite duration segments, in each of which the source conditions are fixed for the duration of the segment.

DRIFT's time-varying model is as follows:

1. The time-varying release is sub-divided into a series of smaller segments using a suitable algorithm (e.g. based on a maximum fractional change between segments);
2. A separate instance of the finite duration model is run for each segment;
3. The concentration profiles from each segment are summed to give an overall time-varying concentration profile.

The time-varying concentration field is expressed as a sum of N separate finite duration segments:

$$C(s_c, t) = \sum_{i=1}^{N} C_{mi}(s_c) P(s_c, s_{i+1}, s_i) \tag{6-11}$$

[24] *In the case that the cloud is delayed by the time to set up steady source, then DRIFT redistributes the material released during this delay period over the whole of the subsequent dispersed cloud*

where we have defined s_{i+1} and s_i to be the front and back ends of segment i and $C_{mi}(s_c)$ is the steady continuous concentration prediction for that segment. For simplicity of presentation (6-11) does not show the interpolation in (6-7), whereas the implementation in DRIFT uses the interpolated form.

A useful property that comes from using the convolution smearing described in Section 6.1 applies when adjacent finite duration segments arise from similar release rates. For this particular case, the front and back end smearing between the adjacent cloud segments adds up in such a way that the overall release approximates to a single finite duration segment of duration equal to the sum of the adjacent segments. We illustrate this by applying (6-6) to (6-11) giving:

$$C(s_c,t) = \overline{C}_m(s_c)P(s_c,s_N,s_1) + \sum_{i=1}^{N} \left(C_{mi}(s_c) - \overline{C}_m(s_c)\right)P(s_c,s_{i+1},s_i) \tag{6-12}$$

where we have used $\overline{C}_m(s_c)$ to represent an 'average' over all the segments of the steady continuous model concentrations. When the variation between segments is sufficiently small, then the second term in (6-12) can be neglected and the concentration field approximated by

$$C(s_c,t) \approx \overline{C}_m(s_c)P(s_c,s_N,s_1) \tag{6-13}$$

Hence we see that, for a sufficiently slowly varying release, the sub-divisions are immaterial and we recover the same result as if we modelled just a single segment over the whole duration. This property is desirable since it offers the possibility of recovering, at least approximately, the steady state limit from modelling a series of sub-divided releases.

Note (6-13) is an approximation which arises when the adjacent segments are similar, however the implementation DRIFT sums the full time dependent concentration profiles from all segments and does not assume that adjacent segments are similar (indeed the segmentation algorithm used to sub-divide a time-varying release is designed to avoid this).

The validity of this type of time-varying model is dependent on dispersion of each finite duration 'step' being independent of the dispersion of the other steps. This is likely to be best approximated when either:

- the release varies sufficiently slowly such that splitting into a small number of separate finite (plume-like) portions does not introduce significant error (similar to making a quasi-steady assumption), or
- the release varies sufficiently rapidly in a distinct portion(s), such that it(they) may be adequately represented by the instantaneous limit of the finite-duration model which disperses effectively independently of the other more slowly varying parts.

It seems likely that the above conditions are best satisfied in, or near, the passive limit where adjacent cloud segments are likely to be travel at similar speeds and are more likely to disperse independently.

The meander time averaging for the time-varying model is as described in Section 5.13, with maximum time for averaging being limited by the total release duration. This means that the same meander averaging time is applied to each segment, irrespective of the duration of that particular segment. For any given release, the plume meander time scale may be longer than a particular segment duration, such that the segment will pass before being repeatedly 'sampled' at a particular location due to meander – in this circumstance the meander time averaging is best regarded as an ensemble average over releases repeated under nominally the same conditions. Such ensemble averaging may be useful for determining toxic dose for use in risk assessments. Another advantage of this approach is that it aids recovering, at least approximately, the results of the time averaged continuous model in the 'steady' limit. Switching off meander time averaging is equivalent to making the pessimistic assumption that the concentration maximum is always sampled.

For segments that differ greatly, 'gaps' may open up between adjacent segments leading to artefacts in the concentration profiles which have arisen due to the discretisation procedure. Increasing the number of segments may in some circumstances help keep gaps at a minimum, but this is at the expense of run time. Also for non-passive releases (dense and buoyant) releases, in general, it is unlikely that many small segments would sum to give the same behaviour as for a single larger segment. Hence, in general, the results from DRIFT's time-varying model will depend upon how a time-varying release is segmented. Ideally segmentation would capture significant features, *e.g.* spikes and long tails in release rate profiles. The segmentation algorithm in DRIFT aims to do this, but is user configurable should further refinement of the segmentation be required.

It is difficult to see how to improve on this approach within an integral model like DRIFT (see e.g. [4] for a discussion of some of the issues in developing a more general time-varying model).

7 THERMODYNAMICS

Thermodynamic modelling in DRIFT v2 is based on the differential homogeneous equilibrium equations given in [71] applied to several specific cases including:

- a two-phase contaminant dispersing in dry air;
- a two-phase contaminant that is immiscible with water dispersing in moist air;
- a two-phase contaminant that forms an ideal solution with water (i.e. obeys Raoult's Law) dispersing in moist air;
- ammonia dispersing in moist air;
- hydrogen fluoride dispersing in moist air.

In the case of ammonia, the heat of interaction and non-ideality of the solution are accounted for. In the case of hydrogen fluoride these are also considered as well as its oligomerisation behaviour.

DRIFT v2 neglected variation of ambient temperature, humidity and pressure. However, to deal with elevated clouds in DRIFT v3 these restrictions are relaxed. We are motivated here by pressure variation due to changing height. Variation of pressure affects the thermodynamic system in two ways:

1. The enthalpy of the mixture changes due to the pressure change;
2. The phase equilibrium is altered by a change in pressure.

In addition to allowing the system pressure to vary, the thermodynamic modelling in DRIFT v3 has been generalised for for multi-component rather than just binary mixtures.

In what follows we present a generalised thermodynamic model that permits any number, N_{liq}, of distinct liquid phases, into which we partition the condensible components of the cloud. All of the components belonging to a particular liquid phase will enter or leave vapour-liquid equilibrium at the same time; but the components of a given liquid phase can enter or leave vapour-liquid equilibrium independently of the components of any of the others. For clarity we introduce the notation that an index i runs over all the components from $1 \dots N_{comp}$; and that an index p runs over the distinct liquid phases from $1 \dots N_{liq}$. The quantity p_i is the index of the liquid phase that component i belongs to. If a component i is condensible then we say that $i \in L$; otherwise $i \notin L$.

We define the following useful quantities:

- z_i is the overall mole fraction of species i;
- y_i is the vapour mole fraction of species i;
- x_i is the liquid mole fraction of species i;
- δ_{pp_i} is unity if species i condenses into liquid phase p and zero otherwise

which can be expressed in terms of the overall moles (or molar fluxes in the continuous model case) via:

$$x_i = \frac{N_{iL}}{N_{L_{p_i}}} \qquad \text{where} \qquad N_{L_{p_i}} = \sum_j N_{jL} \delta_{p_i p_j} \tag{7-1}$$

$$y_i = \frac{N_{iV}}{N_V} \qquad \text{where} \qquad N_{iV} = N_i - N_{iL} \quad and \quad N_V = \sum_i N_{iV} \tag{7-2}$$

$$z_i = \frac{N_i}{N} \qquad \text{where} \qquad N = \sum_i N_i \tag{7-3}$$

where N_{iV} and N_{iL} are the overall number of vapour and liquid moles in the cloud[25]. We also define an overall vapour fraction, V, and liquid fractions for each liquid phase, L_p:

$$L_p = \frac{N_{L_p}}{N} \qquad V = \frac{N_V}{N} \tag{7-4}$$

The x_i, y_i, z_i, L_p and V are related via the following equations:

$$x_i L_{p_i} + y_i V = z_i \tag{7-5}$$

$$\sum_p L_p + V = 1 \tag{7-6}$$

where $L_{p_i}$is defined to equal L_p if substance *i* is present in phase *p* and is zero otherwise.

In order to model the thermodynamics we add the following differential equation to the instantaneous model:

$$N\frac{d\Delta h}{dt} = \dot{Q}_H - \Delta h \dot{N}_{entrain} - h(\dot{N} - \dot{N}_{entrain}) - NU_z\, C_{pa}\frac{d\theta_a}{dz} - \rho_a g(V - v_a N)\, U_z \tag{7-7}$$

and the corresponding equation to the continuous model:

$$\mu\frac{d\Delta h}{ds_c} = Q'_H - \Delta h \mu'_{entrain} - h(\mu' - \mu'_{entrain}) - \mu U_z\, C_{pa}\frac{d\theta_a}{dz} - \rho_a g(\dot{V} - v_a \mu)\, \hat{\mathbf{e}} \cdot \hat{\mathbf{z}} \tag{7-8}$$

where Δh is the difference between the cloud molar enthalpy and the molar enthalpy of the atmosphere and Q_H is the rate of change of molar enthalpy in the cloud due to:

- Material entering the cloud from any source.
- Heat and material loss to the ground from deposition.

The other terms on the right-hand sides of (7-7) and (7-8) arise from the fact that, to minimise subtraction errors, we are considering the rate of change of the *excess cloud enthalpy* compared to the surrounding atmosphere rather than the cloud enthalpy itself.

In order to compute the cloud temperature T we also add the following algebraic constraint:

[25] *Replace these by the corresponding molar fluxes, μ_{iV} and μ_{iL}, in the case of the continuous model.*

$$\Delta h = \sum_i \left[(h_i^L - h_{i,a}^L) x_i L_{p_i} + (h_i^V - h_{i,a}^V) y_i V\right] + \sum_p L_p \, \Delta h_p^{(mix)} \tag{7-9}$$

where h_i^V is the vapour molar enthalpy of component i; h_i^L is liquid molar enthalpy; and the subscript a denotes that the quantity in question should be evaluated for ambient moist air. h_i^V and h_i^L are temperature-dependent quantities. $\Delta h_p^{(mix)}$ is the enthalpy of mixing per mole of liquid for any liquid components present in liquid phase p. $\Delta h_p^{(mix)}$ is zero for ideal mixtures, for non-ideal mixtures, such as Ammonia-Water and Hydrogen Fluoride-Water the binary interaction model of Wheatley is adopted [72].

To encode the effects of pressure variation with height we impose an extra differential equation. For the instantaneous model this takes the form:

$$\frac{dP}{dt} = -\rho_a g \, U_z \tag{7-10}$$

and for the continuous model is:

$$\frac{dP}{ds_c} = -\rho_a g \, \hat{\mathbf{e}} \cdot \hat{\mathbf{z}} \tag{7-11}$$

We also impose an algebraic constraint:

$$h_a(\theta_a, P_{ref}) = h_a(T_a, P) + M_a g z_c \tag{7-12}$$

which relates the ambient potential temperature, θ_a, to the actual ambient temperature, T_a, at the cloud centreline height z_c, which is the z-component of $\mathbf{r_c}$. Here P_{ref} is a reference pressure (usually taken to be standard atmospheric pressure) and M_a is the molar mass of the atmosphere at the cloud centroid height. $h_a(T,P)$ is the molar enthalpy of the ambient mixture at the specified temperature and pressure.

7.1.1 LIQUIDS AND CONDENSATION

Components in the cloud obey one of the following constraints, depending on their phase:

$$y_i = \begin{cases} z_i/\mathrm{V} & \text{Vapour} \\ x_i K_i & \text{Two} - \text{Phase} \qquad i = 1 \ldots N_{comp} \\ 0 & \text{Liquid} \end{cases} \tag{7-13}$$

where

$$K_i = \frac{\gamma_i P_i}{P} \tag{7-14}$$

with γ_i and P_i the liquid activity coefficient and pure vapour pressure of species i respectively. Certain special cases (e.g. Ammonia, Hydrogen Fluoride) adopt the binary model of Wheatley [72] which predicts non-trivial γ_i; but in the majority cases we assume that the mixing is ideal ($\gamma_i = 1$). The following constraint must be met for each liquid phase that is in vapour-liquid equilibrium:

$$\sum_{i=1}^{N_{comp}} x_i \delta_{pp_i} = 1 \qquad p = 1 \dots N_{liq} \tag{7-15}$$

The initial phase composition of the cloud is determined by an isenthalpic flash calculation. This may result in vaporisation of superheated liquid or condensation of subcooled vapour. DRIFT allows also the modelling of subcooled liquid sprays, in which case the model mixes in a small amount of air at the source (as an aid to the numerical solution).

Components belonging to liquid phase p will start to condense when the following condition is met:

$$F_p = \sum_{i \notin L} \frac{z_i}{V} + \sum_{i \in L} \frac{z_i \left(K_i - \delta_{pp_i}\right)}{L_{p_i} + K_i V} = 0 \tag{7-16}$$

A liquid phase that was previously in vapour-liquid equilibrium will dry-out to become a pure vapour phase when all the liquid moles have evaporated.

7.1.2 HYDROGEN FLUORIDE OLIGOMERISATION

DRIFT adopts a so-called ‘1-2-6’ oligomerisation model for hydrogen fluoride in the liquid phase. That is HF vapour is taken to exist as monomer (HF), dimer (H_2F_2) and hexamer (H_6F_6). To model Hydrogen Fluoride we add an extra variable, $y_{HF,1}$, to the set of primary variables, which is the HF monomer vapour mole fraction. We also add the following equation to the equation set to ensure that the oligimer balance is satisfied:

$$\sum_{i=1}^{N_{comp}} y_i = 1 \tag{7-17}$$

Where the overall vapour mole fraction of HF, y_{HF}, is related to the monomer vapour mole fraction via:

$$y_{HF} = y_{HF,1} + a_2(T,P)\, y_{HF,1}^2 + a_6(T,P)\, y_{HF,1}^6 \tag{7-18}$$

This can be thought of in terms of the sum of monomer, dimer and hexamer vapour mole fractions in the cloud, since the dimer, $y_{HF,2}$, and hexamer, $y_{HF,6}$, vapour mole fractions can be expressed as follows:

$$y_{HF,2} = a_2(T,P)\, y_{HF,1}^2 \tag{7-19}$$

$$y_{HF,6} = a_6(T,P)\, y_{HF,1}^6 \tag{7-20}$$

Following Clough et al [73] the a_k are given by:

$$a_k = \left(\frac{P}{P_{ref}}\right)^{k-1} \exp\left[-\frac{1}{R}\left(\frac{\Delta H_k}{T} + \Delta S_k\right)\right] \qquad k = 2{,}6 \tag{7-21}$$

with P_{ref} a reference pressure (taken to be $1\ \mathrm{Nm}^{-2}$) and $R = 8.31\ \mathrm{Jmol}^{-1}\mathrm{K}^{-1}$ the gas constant. ΔS_k and ΔH_k are constants given by:

$$\Delta S_2 = -2.24{\times}10^2\ \mathrm{Jmol}^{-1}\mathrm{K}^{-1} \quad (7\text{-}22)$$
$$\Delta S_6 = -1.023{\times}10^3\ \mathrm{Jmol}^{-1}\mathrm{K}^{-1} \quad (7\text{-}23)$$
$$\Delta H_2 = 3.3076{\times}10^4\ \mathrm{Jmol}^{-1} \quad (7\text{-}24)$$
$$\Delta H_6 = 1.6747{\times}10^5\ \mathrm{Jmol}^{-1} \quad (7\text{-}25)$$

The monomer, dimer and hexamer components have differing vapour molar enthalpies, so the overall vapour molar enthalpy, h_{HF}^V, can be determined using the following relation:

$$y_{HF}\ h_{HF}^V = y_{HF,1}\ h_{HF,1}^V + y_{HF,2}\ h_{HF,2}^V + y_{HF,6}\ h_{HF,6}^V \quad (7\text{-}26)$$

8 DISCUSSION

This report documents the mathematical model implemented in DRIFT v3. DRIFT v3 includes a number of modelling enhancements compared with DRIFT v2. These include:

- Buoyant lift-off and rise;
- Determination of the atmospheric temperature vertical variation from potential temperature and humidity profiles;
- Modification of the vertical concentration profile to match Wheatley's elevated model;
- Allowance for the effect of the vertical variation of atmospheric pressure on the cloud thermodynamics;
- Allowance for the effects of vertical meander in the convective boundary layer;
- Incorporation of a momentum jet model;
- Calculation of initial dilution over the source and upwind spreading;
- Extension of the model to handle finite duration and time-varying releases;
- Generalisation to multi-component mixtures.

The model equations presented modify and extend those in the initial model specification [5] which mainly concerned buoyant lift-off and rise aspects. Some changes have also been made in the light of the comparisons in [74] and [67]. The resulting new version of DRIFT should be more capable of modelling a wider range of scenarios, including dispersion of hydrogen fluoride under low wind humid conditions.

9 ACKNOWLEDGEMENTS

The authors would like to thank David Webber and Simon Coldrick of HSL for their useful comments and discussions on earlier drafts of this report. Thanks also go to Helen Cruse and Alison McGillivray of HSL and also Steve Porter, Harvey Tucker and Rob Dakin of HSE for their feedback and patience during the testing of the DRIFT Version 3 computer implementation. We also acknowledge all those (too numerous to name here) that contributed to the development of the original DRIFT model which provided such a strong starting point for this new work.

10 REFERENCES

[1] D. M. Webber, S. J. Jones, G. A. Tickle and T. Wren, “A model of a dispersing dense gas cloud and the computer implementation D*R*I*F*T. I. Near-instantaneous releases,” UKAEA Report SRD/HSE R586, 1992.

[2] D. M. Webber, S. J. Jones, G. A. Tickle and T. Wren, “A model of a dispersing dense gas cloud and the computer implementation D*R*I*F*T. II. Steady continuous releases,” UKAEA Report SRD/HSE R587, 1992.

[3] S. J. Jones, A. Mercer, G. A. Tickle, D. M. Webber and T. Wren, “Initial verification and validation of DRIFT,” AEA Technology Report SRD/HSE R580, 1993.

[4] D. M. Webber, S. J. Jones, D. Martin, T. GA and T. Wren, “Complex Features in Dense Gas Dispersion Modelling, Vols I and II,” AEA Technology Report AEA/CS/FLADIS/1994 Issue 1, 1994.

[5] G. A. Tickle and J. E. Carlisle, “Extension of the dense gas dispersion model DRIFT to include buoyant lift-off and buoyant rise,” Research Report RR629, Health and Safety Executive, 2008.

[6] S. R. Porter and C. Nussey, “A summary of the URAHFREP project,” Report URAHFREP:PL 971152, Contract ENV4-Ct97-0630, HSE for EC, 2001.

[7] D. J. Hall and S. Walker, “Plume rise from buoyant area sources at the ground,” Client Report No: 80921, BRE, 2000.

[8] D. J. Hall, S. Walker and P. J. Tily, “Puff rise from buoyant area sources at the ground,” Client Report No: 202614, BRE, 2001.

[9] S. R. Ramsdale and G. A. Tickle, “Review of lift-off models for ground based buoyant clouds,” AEA Technology Report AEAT-4262 Issue 2, 2001.

[10] G. A. Briggs, “Lift-off of buoyant gas initially on the ground,” ATDD/NOAA, ATDL Contribution File, No. 87, TN 37831, Oak Ridge , 1973.

[11] S. R. Hanna, G. A. Briggs and J. C. Chang, “Lift-off of ground based buoyant plumes,” *Journal of Hazardous Materials,* vol. 59, pp. 123-130, 1998.

[12] D. J. Hall and R. A. Waters, “Further experiments on a buoyant emission from a building,” Client Report LR 567 (PA), Warren Springs Laboratory, 1986.

[13] D. J. Hall, V. Kukadia, S. Walker and G. W. Marsland, “Plume Dispersion from Chemical Warehouse Fires,” Client Report CR 56/95, Building Research Establishment, 1995.

[14] G. A. Tickle, “Integral modelling of the dilution and lift-off of ground based buoyant plumes and comparison with wind tunnel data,” AEA Technology Report AEAT/NOIL/27328006/001

(R) Issue 2, 2001.

[15] M. Nielsen, "Dense gas dispersion in the atmosphere," Risoe-R-1030(EN), Risoe National Laboratory, 1998.

[16] L. Post, "HGSYSTEM 3.0 Technical Reference," Shell Research, 1994.

[17] S. Ott, "An integral model for continuous HF releases," Risoe-R-1212(EN), Risoe National Laboratory, 2001.

[18] G. A. Tickle, D. Martin and S. A. Ramsdale, "EJECT - An integral model of a two-phase jet in a cross-flow (Theory Manual for EJECT Version 2.01)," AEA Technology Report AEAT-1517 Issue 2, 1998.

[19] G. A. Tickle, "Extending EJECT to model ground based jets," AEA Technology Report AEAT-2369 Issue 1, 1998.

[20] G. A. Briggs, "Plume Rise," in *Atmospheric Science and Power Production*, D. Randerson, Ed., US Department of Energy, 1984.

[21] M. Schatzmann, "An integral model of plume rise," *Atmospheric Environment,* vol. 13, pp. 721-731, 1978.

[22] H. W. Witlox and A. Holt, "A unified unified model for jet, heavy and passive dispersion including droplet rainout and re-evaporation.," in *Internation Conference and Workshop on Modeling the Consequences of Accidental Releases of Hazardus Materials, AIChE*, San Francisco, 1999.

[23] J. Nikmo, J. Tuovinen, J. Kukkonen and I. Valkama, "A hybrid plume model for local-scale dispersion," *Atmospheric Environment,* vol. 33, pp. 4389-4399, 1999.

[24] D. Martin, D. M. Webber, S. J. Jones, B. Y. Underwood, G. A. Tickle and S. A. Ramsdale, "Near- and Intermediate-Field Dispersion from Strongly Buoyant Sources," AEA Technology Report AEAT/1388, 1997.

[25] A. G. Robins, D. D. Apsley, D. J. Carruthers, C. A. McHugh and S. J. Dyster, "Plume Rise Model Specification," CERC Report ADMS 3 P11/02N/05, 2005.

[26] A. J. Cimorelli, S. G. Perry, A. Venkatram, J. C. Weil, R. J. Paine, R. B. Wilson, R. F. Lee, W. D. Peters, R. W. Brode and J. O. Paumier, "AERMOD: Description of Model Formulation," US EPA EPA-454/R-03-004, 2004.

[27] J. M. Richards, "Puff motions in unstratified surroundings," *Journal of Fluid Mechanics,* vol. 21, pp. 97-106, 1965.

[28] J. M. Richards, "Inclined buoyant puffs," *Journal of Fluid Mechanics,* vol. 32, pp. 681-692, 1968.

[29] J. S. Turner, “The motion of buoyant elements in turbulent surroundings,” *Journal of Fluid Mechanics,* vol. 16, pp. 1-16, 1963.

[30] J. S. Turner, “The flow into an expanding spherical vortex,” *Journal of Fluid Mechanics,* vol. 18, pp. 195-208, 1964.

[31] J. S. Turner, “The dynamics of spheroidal masses of buoyant fluid,” *Journal of Fluid Mechanics,* vol. 19, pp. 481-490, 1964.

[32] J. S. Turner, “On the energy deficiency in self-preserving convective flows,” *Journal of Fluid Mechanics,* vol. 53, pp. 217-226, 1972.

[33] J. S. Turner, Buoyancy Effects in Fluids, Cambridge University Press, 1973.

[34] T. K. Fannelop, Fluid Mechanics for Industrial Safety and Environmental Protection, Industrial Safety Series Volume 3 ed., Elsevier, 1994.

[35] E. J. Kansa, “A time-dependent buoyant puff model for explosive sources,” UCRL-ID-128733, Lawrence Livermore National Laboratory, 1997.

[36] M. C. Brown, C. E. Kolb, J. A. Conant, J. Zhang, D. M. Dussault, T. L. Rush, B. E. Conway, J. W. Morris and J. Touma, “Source Characterisation Model (SCM). A Predictive Capability for the Source Terms of Residual Energetic Materials from Burning and/or Detonation Activities. SERDP Project CP-1159 Final Report,” Aerodyn Research Inc. ARI-RR-1384, 2004.

[37] J. X. Zhang, N. A. Moussa, D. E. Groszmann and M. C. Masonjones, “Application of ADORA to Dispersion Modeling of Instantaneously Reacting Chemicals,” in *Proceedings of the Sixth Topical Meeting on Emergency Preparedness and Response American Nuclear Society, April 22-25*, San Francisco, 1997.

[38] D. M. Deaves and C. R. Hebden, “Aspects of Dispersion following an Explosive Release,” ADMLC/2004/3, UK Atmospheric Dispersion Modelling Liaison Committee, 2004.

[39] C. J. Wheatley, “Dispersion of a passive puff released at the ground into the diabatic atmospheric boundary layer,” UKAEA Report SRD/HSE R445, 1988.

[40] J. A. Businger, “Turbulent transfer in the atmosphere,” in *Workshop on Micrometeorology*, 1973.

[41] M. J. Brown, S. P. Arya and S. WH, “Vertical dispersion from surface and elevated releases: An investigation of a non-gaussian plume model,” *Journal of Applied Meteorology,* vol. 32, pp. 490-505, March, 1993.

[42] S. Ott and H. E. Joergensen, “Meteorology and lidar data from the URAHFREP field trials,” Risoe-R-1212(EN), Risoe National Laboratory, 2001.

[43] G. A. Tickle, “Model predictions compared with URAHFREP Campaign 2 Field Trial Data,”

AEA Technology Report AEAT/NOIL/27328006/003 (R) Issue 2, 2001.

[44] M. Nielsen, P. C. Chatwin, H. E. Jorgensen, N. Mole, R. J. Munro and S. Ott, “Concentration fluctuations in gas releases by industrial accidents,” Risoe-R-1329(EN), Risoe National Laboratory, 2002.

[45] D. J. Carruthers, W. S. Weng, J. C. Hunt, R. J. Holroyd, C. A. McHugh and S. J. Dyster, “Plume/Puff Spread and Mean Concentration Module Specifications,” CERC ADMS 3 P10/01T/03, P12/01T/03, 2003.

[46] D. S. Wratt, “An experimental observation of some methods of estimating turbulence parameters for use in dispersion models,” *Atmospheric Environment,* vol. 21, pp. 2599-2608, 1987.

[47] R. J. Yamartino, J. S. Scire, G. R. Carmichael and Y. S. Yang, “The CALGRID mesoscale photochemical grid model - I. Model formulation,” *Atmospheric Environment,* vol. 26A, pp. 1493-1512, 1992.

[48] S. R. Hanna and R. E. Britter, Wind flow and vapour cloud dispersion at industrial and urban sites, CCPS, AIChE, 2002.

[49] H. A. Panofsky and J. A. Dutton, Atmospheric Turbulence, John Wiley and Sons, Inc., 1984.

[50] J. R. Garratt, The Atmospheric Boundary Layer, Cambridge University Press, 1994.

[51] A. J. Byrne, S. J. Jones, S. C. Rutherford, G. A. Tickle and D. M. Webber, “Description of ambient atmospheric conditions for the computer code DRIFT,” UKAEA Report SRD/HSE R533, 1990.

[52] A. C. Beljaars and A. M. Holtslag, “Flux parameterization over land surfaces for atmospheric models,” *Journal of Applied Meteorology,* vol. 30, pp. 327-341, 1991.

[53] S. R. Hanna and R. J. Paine, “Hybrid Plume Dispersion Model (HPDM) Development and Evaluation,” *Journal of Applied Meteorology,* vol. 28, pp. 206-228, 1989.

[54] D. J. Thomson, “The Met Input Module (ADMS 3),” ADMS 3 P05/01N/03, CERC, 2003.

[55] R. H. Clarke, “A model for short and medium range dispersion of radionuclides released to the atmosphere,” NRPB-R91, NRPB, 1979.

[56] P. Seibert, B. F, S. E. Gryning, S. Joffe, A. Rasmussen and P. Tercier, “Mixing Height Determination for Dispersion Modelling,” Report of Work Group 2, EU COST 710 Action on Pre-Processing of Meteorolical Data for Dispersion Modelling, 1997.

[57] D. J. Carruthers and S. J. Dyster, “Boundary Layer Structure Specification,” CERC ADMS 3 P09/01T/03, 2003.

[58] M. Abramowitz and I. A. Stegun, Handbook of Mathematical Functions with Formulas, Graphs, and Mathematical Tables, Dover, 1965.

[59] A. H. Shepherd and D. H. Deaves, “Source Term Calculation for Flashing Releases - Background to the Development of ACE,” WSA Report No. AM5233-R1, WS Atkins, 2000.

[60] G. A. Tickle, “Comparison of DRIFT 3.6.7 Instantaneous Model Predictions with Thorney Island Trials,” ESR Technology Report, ESR/UC000417/001/Draft A, 2013.

[61] A. D. Birch, D. J. Hughes and F. Swaffield, “Velocity decay of high pressure jets,” *Comb. Sci. Tech.,* vol. 52, pp. 161-171, 1987.

[62] C. J. Wheatley, “Discharge of liquid ammonia to moist atmospheres - survey of experimental data and model for estimating the initial conditions for dispersion calculations,” UKAEA Report SRD/HSE 410, 1987.

[63] G. K. Batchelor, An Introduction to Fluid Mechanics, Cambridge University Press, 1988.

[64] B. E. Launder and W. Rodi, “The turbulent wall jet - measurements and modelling,” *Ann. Rev. Fluid Mech.,* vol. 15, pp. 429-459, 1983.

[65] N. Rajaratnam, Turbulent Jets, Elsevier, 1976.

[66] D. M. Webber, G. A. Tickle, T. Wren and J. Kukkonen, “Mathematical modelling of two-phase release phenomena in hazard analysis,” AEA Technology Report SRD/HSE R584, 1992.

[67] G. Tickle, D. Godaliyadde and J. Carlisle, “Comparison of Predictions from the Gas Dispersion Model DRIFT against URAHFREP Data,” Research Report to be published, Health and Safety Executive, 2012.

[68] G. A. Tickle, “Validation Studies for EJECT Version 2,” AEA Technology Report AEAT-3901 Issue 1, 1998.

[69] J. C. Weil, L. A. Corio and R. P. Brower, “A PDF Dispersion Model for Buoyant Plumes in the Convective Boundary Layer,” *Journal of Applied Meteorology,* vol. 36, pp. 982-1003, 1997.

[70] D. L. Ermak, “User's manual for SLAB: An atmospheric dispersion model for denser-than-air releases,” UCRL-MA-105607, Lawrence Livermore National Laboratory, 1990.

[71] D. M. Webber and T. Wren, “A differential phase equilibrium model for clouds, plumes and jets,” UKAEA Report SRD/HSE R552, 1990.

[72] C. J. Wheatley, “A theory of heterogeneous equilibrium between vapour and liquid phases of binary systems and formulae for the partial pressures of HF and H2O vapour,” UKAEA Report SRD/HSE R357, 1986.

[73] P. N. Clough, D. R. Grist and C. J. Wheatley, “Thermodynamics of mixing and final state of a mixture formed by the dilution of anhydrous hydrogen fluoride with moist air,” UKAEA Report SRD/HSE R396, 1987.

[74] G. Tickle and J. Carlisle, “Comparison of DRIFT Version 3 Predictions DRIFT Version 2 and Experimental Data,” ESR Technology Report ESR/D1000846/STR01/Issue 3, 2012.

APPENDIX A TOXICITY AND FLAMMABILITY OF MULTI-COMPONENT CLOUDS

This Appendix documents the methods used to DRIFT to derive flammability limits and toxicity for multi-component clouds.

A.1 FLAMMABILITY

Flammability of limits of mixtures are determined using *Le Chatelier's Mixing Rule*. The lower flammable limit, LFL, of a multi-component mixture is given by:

$$LFL = \frac{\sum_{i \in \mathcal{F}} z_i}{\sum_{i \in \mathcal{F}} \frac{z_i}{LFL_i}} \tag{A-1}$$

where LFL_i is the lower flammable limit of the pure component i and the notation $i \in \mathcal{F}$ signifies that the sum only applies to those components that are flammable. All concentrations in the above are on a mol/mol basis. The formula for the upper flammable limit is directly analogous.

To assess whether a particular mixture exceeds LFL, the mol/mol mixture concentration is considered as a fraction, z_{LFL}, given by:

$$z_{LFL} = \frac{\sum_{i \in \mathcal{F}} z_i}{LFL} = \sum_{i \in \mathcal{F}} \frac{z_i}{LFL_i} \tag{A-2}$$

If $z_{LFL} > 1$ then the mixture exceeds LFL.

A.2 TOXICITY

For each component we can input a concentration (dose) corresponding to a specified level of harm, C_i (D_i) and combine these in DRIFT using a defined rules-set[26].

One possible way of combining toxicities is to define an overall toxic fraction, z_{toxic} from:

$$z_{toxic} = \sum_{i \in \mathcal{T}} \frac{z_i}{C_i} \tag{A-3}$$

where $i \in \mathcal{T}$ signifies that the sum only applies to those components that are toxic. $z_{toxic} > 1$ indicates that the mixture exceeds the specified level of harm.

A similar relation can be used to quantify multi-component dose:

$$d_{toxic} = \sum_{i \in \mathcal{T}} \frac{d_i}{D_i} \tag{A-4}$$

with d_i is the dose contribution from component i, which is of the form:

[26] *Clearly, toxic response is sufficiently complex that, where possible, toxicity for mixtures should be based upon experimental data rather than mathematical constructs.*

$$d_i = \int z_i^{n_i} dt \tag{A-5}$$

where n_i is the toxic exponent of component i. An alternative for toxic dose is:

$$d_{toxic} = \sum_{i \in \mathcal{T}} \left[\frac{d_i}{D_i}\right]^{1/n_i} \tag{A-6}$$

This has the advantage that, for multiple components with similar or the same toxicity (same or similar target level D_i and exponent n_i), similar, or the same, results would be obtained using multi-components as would be found using a single component with the same toxicity. This would only be true in (A-4) if $n_i = 1$ and for other circumstances, e.g. $n_i = 2$, (A-4) might be considered non-cautious.

Although some interpretation might be attached to $z_{toxic} = 1$, other values of z_{toxic} do not have a clear meaning in either case, apart from being greater than or less than the target value of 1.

APPENDIX B WHEATLEY'S PASSIVE PUFF MODEL

B.1 SUMMARY OF THE MODEL

In Appendix 6 of [39] Wheatley shows how his ground-based passive puff model can be extended to an elevated point source. We do not repeat his analysis here, but pull out some of the key results and show how with minor modification this might be incorporated within DRIFT to allow treatment of elevated passive releases.

[39] presents an approximate solution to the diffusion equation

$$\frac{\partial C}{\partial t} + U(z)\frac{\partial C}{\partial x} = \frac{\partial}{\partial z}K(z)\frac{\partial C}{\partial Z} \tag{B-1}$$

with the following boundary conditions

$$C \to 0 \qquad z \to \infty \tag{B-2}$$
$$C \to 0 \qquad x \to \pm\infty \tag{B-3}$$
$$K\frac{\partial C}{\partial z} \to 0 \qquad z \to 0 \tag{B-4}$$
$$C \to \delta(z_c)\delta(x) \qquad t \to 0 \tag{B-5}$$

representing a point source at elevation z_c in a semi-infinite atmosphere with no flux from/to the ground.

Ordinary differential equation solutions may be obtained by the method of moments - multiplying by products of powers of x and z and integrating over all space.

[39] defines a longitudinal coordinate ξ relative to the leaning cloud axis

$$\xi = x - \langle x \rangle + \zeta(z - \langle z \rangle) \tag{B-6}$$

with ζ the tangent of the angle between the cloud axis and the vertical.

Power law profiles for the variation of K and U with height are assumed:

$$K = K_0 z^m \qquad U = U_0 z^n \tag{B-7}$$

and the concentration distribution is taken to be approximately separable

$$C = C_{\xi 0} C_{0z} \tag{B-8}$$

Wheatley gives the following solutions for the concentration field

$$C_{\xi 0} = \frac{1}{\sqrt{2\pi}\sigma_\xi}\exp\left(\frac{-\xi^2}{2\sigma_\xi^2}\right) \tag{B-9}$$

and

$$C_{0z} = \frac{(z_c z)^{(s-2)/2}}{s\tau} I_{-\nu}\left(\frac{2(z_c z)^{s/2}}{s^2\tau}\right)\exp\left(-\frac{z_c^s + z^s}{s^2\tau}\right) \tag{B-10}$$

where

$$s = 2 - m \ , \qquad \nu = 1 - 1/s \ , \qquad \tau = K_0 t \qquad \text{(B-11)}$$

$I_{-\nu}$ is the modified Bessel function of the first kind of order $-\nu$.

The solutions for the cloud motion and growth involve moments of C_{0z}

$$\begin{aligned}\langle z^q \rangle = H_q &= \int_0^\infty z^q C_{0z} dz \\ &= (s^2\tau)^{q/s} \frac{\Gamma((q+1)/s)}{\Gamma(1/s)} M(-q/s, 1/s, -z_c^s/(s^2\tau))\end{aligned} \qquad \text{(B-12)}$$

$M(a, b, z)$ is the confluent hypergeometric function. $H_0 = 1$ by virtue of the normalisation of the concentration.

The centroid motion is given by

$$\frac{d\langle z \rangle}{dt} = -\int_0^\infty K \frac{\partial C_{0z}}{\partial z} dz \qquad \text{(B-13)}$$

$$= m K_0 H_{m-1} \qquad \text{(B-14)}$$

$$\frac{d\langle x \rangle}{dt} = -\int_0^\infty U C_{0z} dz \qquad \text{(B-15)}$$

$$= U_0 H_n \qquad \text{(B-16)}$$

The cloud growth and leaning is given by

$$\sigma_z \frac{d\sigma_z \zeta}{dt} = -\int_0^\infty (z - \langle z \rangle) U C_{0z} dz - \zeta \int_0^\infty K C_{0z} dz \qquad \text{(B-17)}$$

$$= U_0 (H_{n+1} - H_1 H_n) - \zeta K_0 H_m \qquad \text{(B-18)}$$

$$\sigma_\xi \frac{d\sigma_\xi}{dt} = \zeta^2 \int_0^\infty K C_{0z} dz + \sigma_{\xi 0} \frac{d\sigma_{\xi 0}}{dt} \qquad \text{(B-19)}$$

$$= \zeta^2 K_0 H_m + \sigma_{\xi 0} \frac{d\sigma_{\xi 0}}{dt} \qquad \text{(B-20)}$$

$d\sigma_{\xi 0}/dt$ represents the rate of direct longitudinal diffusion.

The standard deviation σ_z of the vertical concentration distribution is given by

$$\sigma_z^2 = \langle z^2 \rangle - \langle z \rangle^2 = H_2 - H_1^2 \qquad \text{(B-21)}$$

Lateral diffusion is represented by a Gaussian distribution with standard deviation σ_y

$$C_{0y} = \frac{1}{\sqrt{2\pi}\sigma_y} \exp\left(\frac{-y^2}{2\sigma_y^2}\right) \qquad \text{(B-22)}$$

$d\sigma_y/dt$ and $d\sigma_{\xi 0}/dt$ are related to the atmospheric turbulent velocity fluctuations σ_v and σ_u

$$\frac{d\sigma_y}{dt} = 0.3\sigma_v \ , \qquad \frac{d\sigma_{\xi 0}}{dt} = 0.3\sigma_u \tag{B-23}$$

It is straightforward to show that in the limit $z_c \to 0$ the above solution tends to that for DRIFT's ground-based passive model [39]. It can also be shown that the solution results in a reflected Gaussian profile in the limit of constant K and U. In Section B.5 we show how, at least in principle, solutions may be obtained in the circumstance of finite fluxes at the upper and lower boundaries.

B.2 INCORPORATING AS THE PASSIVE LIMIT IN DRIFT

We wish to define concentration profiles of the form

$$c(x, y, z, t) = C_m(t)F_h(\xi, y)F_v(z)$$

with

$$F_h(0,0) = F_v(z_c) = 1 \tag{B-24}$$

so that C_m is the concentration at location $r_c = (x_c, y_c = 0, z_c)$.

To match with the elevated passive puff model we define the vertical profile function

$$F_v(z) = C_{0z}(z)/C_{0z}(z_c) = \tilde{F}_v(\hat{z})/\tilde{F}_v(\hat{z}) \tag{B-25}$$

with

$$\tilde{F}_v(\hat{z}) = s(\hat{z}_c\hat{z})^{(s-1)/2} I_{-v}\big(2\,(\hat{z}\hat{z}_c)^{s/2}\big)\exp(-\hat{z}_c^s - \hat{z}^s) \tag{B-26}$$

$$\hat{z} = z/a_3 \tag{B-27}$$

$$\hat{z}_c = z_c/a_3 \tag{B-28}$$

where we have defined the vertical length scale a_3 by substituting

$$a_3^s = s^2\tau = s^2 K_0 t \tag{B-29}$$

in (B-10).

Taking the reference height for K and U to be the centroid height $Z = \langle z \rangle$, the power law profile may be written

$$K_0 = K_z/Z^m \qquad U_0 = U_z/Z^n \tag{B-30}$$

where K_z and U_z are the diffusivity and wind speed at height Z. Hence

$$a_3^s = s^2 K_z Z^{(s-2)} \tag{B-31}$$

The effective cloud height is

$$H = \int_0^\infty F_v dz = \frac{a}{\tilde{F}_v(\hat{z}_c)} \tag{B-32}$$

Moments $\langle z^q \rangle$ of F_v are given by (B-12).

We can gain some insight into the behaviour of H by considering the constant K and U limit. In this case $H \to \pi^{1/2} a_3$ when elevated ($z_c \to \infty$) and $H \to \pi^{1/2} a_3/2$ when grounded ($z_c \to 0$). This behaviour is useful when it comes to defining a 'top' entrainment velocity from the identity

$$u_T(passive) = \frac{dH}{dt} \tag{B-33}$$

Defining H by (B-32) ensures that for the same da_3/dt, $u_T(passive)$ has approximately twice the value when elevated compared with when grounded. Hence the profile effectively accounts for the geometrical factor of mixing being able to occur through both the top and bottom faces of the cloud when elevated, but only the top when grounded.

From (B-32) and (B-31) an approximate expression for $u_T(passive)$ is

$$u_T(passive) = \frac{1}{\tilde{F}_v(\hat{z}_c)} \frac{da_3}{dt} \tag{B-34}$$

where we have neglected the time derivative of $\tilde{F}_v(\hat{z}_c)$. For a constant z_c, the time derivative $\tilde{F}_v(\hat{z}_c)$ is zero for ground-based clouds, it is also small for very elevated clouds. Hence neglect of this term appears reasonable when seeking an approximate interpolation between these regimes. Neglecting the time derivative when z_c itself varies is more difficult justify [27]. We choose to neglect this term because it is difficult to see how a change in z_c with no change in a_3 could constitute dilution of the cloud. Also neglecting the time derivative of shape terms is consistent with DRIFT's formulation.

We may determine da_3/dt from (B-31)

$$\frac{da_3}{dt} = \frac{sK_z}{Z} \left(\frac{Z}{a_3}\right)^{s-1} \tag{B-35}$$

The horizontal concentration profile function is

$$F_h(\xi, y) = \exp\left[-((\xi/a_1)^2 + (y/a_2)^2)^{w/2}\right] \tag{B-36}$$

with a_1 and a_2 being the length scales in the horizontal and vertical directions which is exactly the same as for the ground-based DRIFT [1]. The passive limit corresponds to $w \to 2$. The effective cloud area A and effective half-axes R_1 and R_2 are unchanged from [1] as are the relations between R_j and σ_j ($j = 1,2$). The spreading velocities are

$$U_2(passive) = \frac{dR_2}{dt} = \frac{2\Gamma(1 + 2/w)}{[\Gamma(1 + 4/w)]^{1/2}} 0.3\sigma_v \tag{B-37}$$

which is also unchanged. However γ_1 in

$$U_1(passive) = \frac{dR_1}{dt} = \frac{2\Gamma(1 + 2/w)}{[\Gamma(1 + 4/w)]^{1/2}} \frac{d\sigma_\xi}{dt}$$

[27] *Strictly the source height should be constant for the passive model to be applied.*

$$= \frac{4[\Gamma(1+2/w)]^2}{\Gamma(1+4/w)} \frac{1}{R_1} \left[\gamma_1 \zeta^2 K_z + 0.3\sigma_{\xi 0}\sigma_u\right]$$

differs and is given by

$$\gamma_1 = \frac{H_m}{H_1^m} = \frac{\Gamma((3-s)/s)[\Gamma(1/s)]^{1-s}}{[\Gamma(2/s)]^{2-s}} \frac{M(2/s-1,1/s,-\hat{z}_c^s)}{[M(-1/s,1/s,-\hat{z}_c^s)]^{2-s}} \quad \text{(B-38)}$$

B.3 CLOUDS WITH VERTICAL EXTENT LESS THAN CENTROID HEIGHT

A limitation of K-theory models, such as Wheatley's passive puff model is that K-theory is inappropriate when the cloud extent (in this case vertical extent) is less than the characteristic eddy size implied by the diffusivity (in this case the height above the ground). This is not a problem for a ground-based puff where the centroid height (at which K is determined) grows with the depth of the cloud. However, this is a problem for an elevated cloud where the centroid height is determined by factors other than the growth in depth. A way around this is to revert to an alternative passive model when z_c/a_3 grows larger than 1. This somewhat negates the usefulness of the elevated passive puff model given in the previous section. However, the K-theory elevated puff model might still provide a useful framework, since in the limit of constant K and U with height it yields Gaussian dispersion. In this case we can specify the vertical growth by noting the following correspondence between K_z and σ_z

$$K_z = \sigma_z \frac{d\sigma_z}{dt} \quad \text{(B-39)}$$

Hence, we can use an alternative model for σ_z e.g. as a function of travel time, to specify K_z and da_3/dt for use with the elevated passive model.

B.4 APPLICATION TO ATMOSPHERIC LAYERS ABOVE THE SURFACE LAYER

The vertical concentration profile shape depends upon the parameter s which is related by (B-11) to the power law index of diffusivity m. Further general profiles of K and U are incorporated by fitting to the centroid height values using (B-30). The accuracy of this approximation relies on the profiles of K and U changing only slowly with height. Section 3 gives profiles of K and U based on scaling models of the atmospheric boundary layer above the surface layer. Although the profiles of K and U given in in Section 3 are continuous, their gradients may be discontinuous at boundaries between layers. Such discontinuous changes in gradient would lead to a discontinuous change in the profile parameters resulting in an undesirable instantaneous change in shape for the *whole* vertical concentration profile. A possible way to smooth over such discontinuities by determining s from

$$s = \frac{\sum_i s_i \Delta z_i}{\sum_i \Delta z_i} \quad \text{(B-40)}$$

where Δz_i is the thickness of layer i (the whole layer thickness if the centroid height Z is above the top of the layer, otherwise the thickness in the layer up to Z), s_i is a representative value for the layer (determined from (B-11) using *m* determined from the gradient near the top of the layer if Z is above the top of the layer, otherwise from the gradient at Z).

B.5 ALLOWING FOR DIFFERENT FLUX CONDITIONS AT UPPER AND LOWER BOUNDARIES

A general solution for the diffusion equation (B-1) is [39]:

$$C_{0z} = \sum_{\forall\lambda} (A_\lambda J_\nu(Y_\lambda) + B_\lambda J_{-\nu}(Y_\lambda)) z^{s\nu/2} e^{-\lambda\tau} \tag{B-41}$$

where:

$$Y_\lambda = \frac{2\sqrt{\lambda}}{s} z^{s/2} \ , \qquad \tau = K_0 \tau \ , \qquad \nu = 1 - 1/s \tag{B-42}$$

The values of λ are determined from the boundary conditions. In the case of the semi-infinite regime studied earlier, λ takes a continuum of positive values and can be integrated out via a Laplace transform to yield the profile given in (B-10). More generally, values of λ will form a series of discrete values, parameterised by an integer, n. In this more general case the concentration profile will take the form:

$$C_{0z} = \sum_{n} (A_n J_\nu(Y_n) + B_n J_{-\nu}(Y_n)) z^{s\nu/2} e^{-\lambda_n\tau} \tag{B-43}$$

with:

$$Y_n = \frac{2\sqrt{\lambda_n}}{s} z^{s/2} \tag{B-44}$$

In this section we are interested in the atmospheric boundary layer height h above the surface of the ground. We wish to allow only a limited amount of material to penetrate this boundary. In addition, we allow deposition of material into the ground itself. The appropriate boundary conditions are:

$$\lim_{z\to 0}\{z^m C'_{0z} - v_- C_{0z}\} = 0 \tag{B-45}$$

$$h^m C'_{0z}|_{z=h} - v_+ C_{0z}|_{z=h} = 0 \tag{B-46}$$

where $'$ denotes d/dz, h is the height of the boundary layer and $m = 2 - s$. The initial condition is the same as in the earlier case:

$$\lim_{t\to 0} C_{0z} = \delta(z - z_c) \tag{B-47}$$

Imposing these boundary conditions yields the three equations. The first of these can be used to solve for the λ_n:

$$\sqrt{\lambda_n} h^{1/2} C'_{n\nu}(Y_{nh}) + \left[\frac{s-1}{2} h^{-(s-1)/2} - v_+ h^{(s-1)/2}\right] C_{n\nu}(Y_{nh}) = 0 \tag{B-48}$$

where:

$$C_{n\nu} = A_n J_\nu + B_n J_{-\nu} \ , \qquad Y_{nh} = \frac{2\sqrt{\lambda_n} h^{s/2}}{s} \tag{B-49}$$

The next equation relates A_n and B_n:

$$A_n = \frac{B_n v_-}{s-1} \frac{\Gamma(1+\nu)}{\Gamma(1-\nu)} \left(\frac{s^2}{\lambda_n}\right)^\nu \tag{B-50}$$

The final equation can be used to solve for B_n (and hence A_n) directly for a given solution of (B-48):

$$[v_+ h^{s-1}(v_+ h^{s-1} + 1 - s) + \lambda_n h^s] C_{n\nu}^2(Y_{nh}) = \lambda_n s z_c^{(s-1)/2} C_{n\nu}(Y_{n z_c}) \tag{B-51}$$